Organic Geochemistry 64 (2013) 58–75

Contents lists available at ScienceDirect

Organic Geochemistry

journal homepage: www.elsevier.com/locate/orggeochem

Hydrocarbon generation from coal, extracted coal and bitumen rich coal in confined pyrolysis experiments

Erting Li, Changchun Pan *, Shuang Yu, Xiaodong Jin, Jinzhong Liu

State Key Laboratory of Organic Geochemistry, Guangzhou Institute of Geochemistry, Chinese Academy of Sciences, Wushan, Guangzhou 510640, China

ARTICLE INFO

Article history:
Received 6 February 2013
Received in revised form 29 August 2013
Accepted 5 September 2013
Available online 13 September 2013

ABSTRACT

Three sets of pyrolysis experiments were performed on extracted coal (R_o% 0.39), coal (initial bitumen 13.5 mg/g coal) and bitumen enriched coal (total bitumen 80.9 mg/g coal) at two heating rates of 2 °C/h and 20 °C/h in confined systems (gold capsules). For all three experiments, the yields of bitumen, Σn-C_{8+}, aromatic components and ΣC_{2-5} at first increase and then decrease with increasing EASY%R_o and reach the highest values within the EASY%R_o ranges of 0.67–1.08, 1.07–1.19, 1.46–1.79 and 1.46–1.68, respectively. In contrast, $C_1/\Sigma C_{1-5}$ ratio at first decreases and then increases with EASY%R_o and reaches a minimum value in EASY%R_o range of 0.86–1.08, closely corresponding to the maximum values of the yields of bitumen and Σn-C_{8+}. Methane yields increase consistently with EASY%R_o. Nearly half of the maximum yield of methane from kerogen was generated at EASY%R_o > 2.2. The differences in methane yields among the three experiments at the same thermal stress are relatively minor at EASY%R_o < 2.2, but are greater with thermal stress at EASY%R_o > 2.2. This demonstrates that the kerogen always retained relatively more hydrogen and hydrocarbon generative potential at the postmature stage of bitumen rich coal than the extracted coal or coal.

The maximum yield of ethane is 20–25% higher in the bitumen rich coal experiment than the extracted coal or coal, while the maximum yields of C_3, C_4 and C_5 in the former are double to triple those in the latter. This result demonstrates that the added bitumen in bitumen rich coal substantially increased the generation of these wet gases. However, the averaged values of activation energies (with the same frequency factors) for both the generation and cracking of individual wet gases are similar and do not show consistent trends among the three experiments. For all three experiments, activation energies for the generation and cracking of wet gases are significantly lower than those in previously published oil pyrolysis experiments with same frequency factors (Pan et al., 2012; Organic Geochemistry 45, 29–47). Methane $\delta^{13}C$ values at the maximum temperature or EASY%R_o are close to those of initial wet gases, especially C_3, implying that the major part of methane shared a common initial precursor with wet gases, i.e., free and bound liquid alkanes.

1. Introduction

Coals are important source rocks for hydrocarbon gases in sedimentary basins. Dai et al. (2008) indicate that the hydrocarbon gases in most giant gas fields discovered in China are dominantly derived from coal source rocks. However, the generation of hydrocarbon gases from humic coals is complex and poorly understood. Numerous studies have documented the interaction between kerogen and oil or bitumen (e.g., Boreham et al., 1999; Mansuy et al., 1995; McNeil and BeMent, 1996). McNeil and BeMent (1996) proposed a mechanism for the formation of hydrocarbon gases from oil cracking in source rocks where alkane moieties attached to aromatic rings in kerogen cleave at the position between the first and second carbon atoms. As a result, methane is the dominant hydrocarbon gas. Boreham et al. (1999) suggested that the generation of volatile hydrocarbons is accompanied by partial reincorporation of the free hydrocarbons and bitumen into kerogen during natural maturation of coal.

Mansuy et al. (1995) demonstrated that pyrolysates (hydrocarbons and polar components) released from kerogen react with each other and with the kerogen and emphasized that the reaction medium is important for hydrocarbon formation from kerogen in confined pyrolysis experiments on coal. However, gas products were not investigated in their study. Erdmann and Horsfield (2006) suggested that the recombination reactions of liquid products released from type III kerogen at low levels of maturation result in the formation of a thermally stable bitumen, which is the major source of methane at very high maturity based on non-isothermal closed (microscale sealed vessel) and open pyrolysis studies. Vu et al. (2008) observed that the yields and compositions of gas and liquid hydrocarbons are significantly different between extracted and

* Corresponding author. Tel.: +86 20 85290183; fax: +86 20 85290706.
E-mail address: cpan@gig.ac.cn (C. Pan).

0146-6380/$ - see front matter © 2013 Elsevier Ltd. All rights reserved.
http://dx.doi.org/10.1016/j.orggeochem.2013.09.004

non-extracted New Zealand coals in open system pyrolysis using Rock–Eval and pyrolysis–gas chromatography. They suggested that second order reactions between kerogen and bitumen during pyrolysis reduce primary gas yield and enhance both oil and secondary gas yield (Vu et al., 2008).

Previous studies suggested that humic coals with generative potential < 200 mg/g TOC are capable of expelling gas/gas-condensate only (e.g., Pepper, 1992; Sandvik et al., 1992; Pepper and Dodd, 1995; Pepper and Corvi, 1995). Hydrocarbon generation from humic coal and the interaction between bitumen or hydrocarbons and solid kerogen can be simulated using a confined pyrolysis system (gold capsules) as developed by Monthioux et al. (1985, 1986). The purpose of this paper is to use non-isothermal closed system pyrolysis on coal, extracted coal and bitumen enriched coal (bitumen added) to evaluate (1) the influence of initial bitumen content on liquid and gaseous hydrocarbon yields, (2) their chemical and isotopic compositions, and (3) hydrocarbon gas kinetic parameters for primary and secondary cracking.

2. Samples and experimental

2.1. Samples

The coal was collected from Jurassic strata in Jilin Province, northeastern China. The coal was first ground to powder (about 200 mesh). The vitrinite reflectance (R_o%), organic elemental compositions (CHON), $\delta^{13}C$ value, Rock–Eval parameters and bitumen content for this coal are listed in Table 1. A portion of coal powder (51.61 g) was Soxhlet extracted with benzene:methanol (9:1 v:v) for 72 h. After Soxhlet extraction, 139 ml of bitumen solution was obtained. A small portion of this (2.0 ml) was dried using a stream of N_2 for bitumen quantification. The bitumen (10.0 mg) was first diluted with about 0.1 ml dichloromethane and then deasphaltened using 40× excess of hexane. The deasphaltened sample was fractionated on a silica:alumina column using hexane, benzene and methanol as eluants to yield the saturate, aromatic and resin fractions, respectively. The remaining 137 ml of bitumen solution was mixed with another portion of coal powder (9.33 g). Most solvent in the mixed sample was removed by rotary evaporation. The mixed sample was left open to the air for a week to remove the remaining solvent. Finally, three types of samples, i.e. coal (primary bitumen = 13.5 mg/g coal), extracted coal (without bitumen) and coal plus bitumen (total bitumen = 80.9 mg/g coal) were prepared for pyrolysis experiments.

2.2. Confined pyrolysis experiments

2.2.1. Gold capsules and sample loading

All pyrolysis experiments on coal, extracted coal and bitumen rich coal were conducted in flexible gold capsules (4 mm o.d., 0.25 mm wall thickness and 40 mm length) contained within steel pressure vessels. The capsules were welded at one end before being loaded with samples. Each capsule was loaded with 10–60 mg sample. Once loaded, the open end of each capsule was purged with argon before being squeezed in a vise to create an initial seal, which was subsequently welded in the presence of argon. During welding, the previously welded end was submerged in cold water to prevent heating of reactants.

2.2.2. Pyrolysis apparatus

Our experimental system permits 14 pressure vessels to be placed in a single furnace. A fan at the bottom of the furnace keeps the vessels at the same temperature during the experiment. The vessels were previously filled with water. Three capsules containing coal, extracted coal and coal plus bitumen were placed together in each vessel. The internal pressure of the vessels, connected to each other with tubing, was adjusted to 50 MPa by pumping water into the vessels before heating. This pressure was used in consideration of both the geological conditions and safety. It was maintained automatically by pumping water into or out of the vessels during pyrolysis experiments. The error of the pressure is < ± 0.1 MPa.

Two heating programs were used for the pyrolysis experiments, 2 °C/h and 20 °C/h. The vessels were heated to 250 °C within 10 h, and then from 250 °C to 600 °C at a rate of 2 °C/h or 20 °C/h. Two thermocouples were used to measure the temperature of the pyrolysis experiments and to check each other. One thermocouple was attached to the outside wall of a vessel to record oven temperatures. The other thermocouple was placed inside this vessel to record the temperature of the samples. The former temperatures were slightly higher than the latter with a difference < 0.5 °C. The error of the recorded temperatures is < 1 °C. Vessels containing gold capsules were removed from the oven at temperature intervals of 12 °C or 24 °C between 336 °C and the final temperature. Each vessel was quenched to room temperature in cold water within 10 min.

After the first run of each heating experiment, the capsules were cleaned, dried and weighed. Unfortunately, a large number of capsules leaked because their weight before and after the heating experiment differed by > 5 mg. For capsules without leakage, weight differences were < 0.05 mg. Therefore, a second run of the pyrolysis experiment was performed. The data obtained from the second run are in Table 2.

2.3. Chemical and carbon isotopic analyses of gas components

After pyrolysis, the volatile components in the capsules were collected in a special sampling device connected to an Agilent 6890 N GC modified by Wasson ECE Instrumentation as described previously (Pan et al., 2006, 2008, 2010, 2012). Briefly, the whole device was at first evacuated to < 1×10^{-2} Pa. The gold capsule was then pierced with a needle, allowing the gases to escape into the device. The valve connecting the device and the modified GC was open to allow the gas to enter the GC. The GC analyses of both the organic and inorganic gas components were performed in an automatically controlled procedure. The oven temperature for the hydrocarbon gas analysis was initially held at 70 °C for 6 min, ramped from 70 to 130 °C at 15 °C/min, from 130–180 °C at 25 °C/min, and then held at 180 °C for 4 min. For the inorganic gas analysis, the oven temperature was held at 90 °C. The analysis of all gases was carried out from one injection. A test with external standard gases indicated that the amounts of gas products measured using this device had < 0.5% relative error.

After GC analysis, the remaining gas components trapped within the device (about 80% of the initial amount) were taken for gas chromatography–isotope ratio mass spectrometry (GC–IRMS) using a syringe to pierce the septum of the device. This analysis

Table 1
Gross geochemical parameters for the coal.

R_o%	C%	H%	O%	N%	$\delta^{13}C$‰	S1	S2	HI	OI	*T*max	Bit
0.391	69.94	5.20	16.88	0.83	−22.86	4.27	121.80	174	11.18	427	13.5

S1 and S2: in mg/g coal; HI and OI: in mg/g TOC; *T*max: in °C; Bit: bitumen: in mg/g coal, obtained by Soxhlet extraction using dichloromethane:methanol (93:7 v:v) for 72 h.

Table 2
Amounts of bitumen, *n*-alkanes, aromatic components and gas components produced during coal pyrolysis experiments (mg/g coal).

T (°C)	EASY%R_o	Coal (mg)	Bit	Σ*n*-C_{8+}	Aro	C_1	C_2H_6	C_2H_4 × 10^{-3}	C_3H_8	C_3H_6 × 10^{-3}	*i*-C_4 × 10^{-2}	*n*-C_4 × 10^{-2}	*i*-C_5 × 10^{-2}	*n*-C_5 × 10^{-2}	H_2 × 10^{-2}	CO_2	ΣC_{1-5}	ΣC_{1-5} (ml/g coal)	$C_1/\sum C_{1-5}$ (wt)
Extracted coal (20 °C/h)																			
335.6	0.57	59.25	29.54	0.357	0.605	0.11	0.020	0.32	0.009	0.50	0.13	0.10	–	–	0.00	19.77	0.14	0.19	0.767
360.4[a]	0.68	60.08	34.80	0.497	0.828	0.69	0.159	1.65	0.066	1.77	0.93	–	–	–	0.36	36.06	0.93	1.23	0.744
383.7	0.79	50.59	55.54	1.955	2.381	0.74	0.341	1.00	0.167	2.21	2.03	1.56	0.23	0.12	0.33	34.45	1.29	1.52	0.573
407.3	0.95	46.09	50.12	4.130	3.160	1.94	1.105	3.01	0.575	7.90	6.81	7.00	0.98	0.46	1.30	45.23	3.78	4.26	0.512
420.2[a]	1.06	47.61	52.93	4.441	4.250	7.90	4.280	4.92	2.251	15.67	33.81	36.42	10.20	5.35	4.41	65.62	15.31	17.21	0.516
432.2[a]	1.19	45.03	51.74	4.458	5.256	11.08	5.557	4.73	2.770	15.84	37.11	41.65	9.84	5.22	5.60	70.00	20.37	23.45	0.544
455.2	1.46	37.17	31.48	1.100	7.070	16.48	7.043	5.30	3.396	22.18	46.57	53.68	9.97	5.74	5.36	59.86	28.11	33.38	0.586
468.1[a]	1.63	37.88	35.37	0.367	7.988	23.34	8.634	8.71	3.653	31.57	61.43	59.62	15.75	7.50	9.74	78.57	37.11	45.45	0.629
479.4	1.79	32.92	18.81	–	8.217	30.25	8.358	8.81	2.557	23.59	35.35	17.66	1.97	0.55	7.57	68.02	41.75	54.82	0.724
494.3[a]	2.03	32.77	16.99	–	8.471	36.19	8.857	15.92	2.425	28.13	43.36	18.93	2.67	0.77	13.10	85.03	48.17	64.30	0.751
503.4	2.18	28.33	ND	ND	ND	40.05	7.101	8.19	1.015	9.70	8.64	1.09	–	–	14.26	71.11	48.28	67.74	0.829
504.5[a]	2.20	36.34	ND	ND	ND	41.36	7.773	11.14	1.382	149.46	20.96	4.06	–	–	15.50	82.36	50.92	70.65	0.812
516.0[a]	2.40	28.25	ND	ND	ND	49.84	6.384	6.41	0.486	5.05	2.88	–	–	–	21.21	94.63	56.75	81.82	0.878
527.6	2.60	23.88	ND	ND	ND	62.09	4.897	9.23	0.172	2.90	1.30	–	–	–	25.75	88.75	67.18	99.18	0.924
527.9[a]	2.61	26.04	ND	ND	ND	55.78	4.381	8.59	0.231	3.50	2.27	–	–	–	25.77	94.55	60.42	89.14	0.923
551.5	3.05	19.74	ND	ND	ND	62.69	2.112	3.82	0.022	–	–	–	–	–	32.32	86.04	64.83	97.74	0.967
551.9[a]	3.06	20.76	ND	ND	ND	65.36	2.486	7.69	0.059	–	–	–	–	–	38.43	97.21	67.91	102.15	0.962
575.3	3.48	14.74	ND	ND	ND	71.35	1.372	3.07	0.012	–	–	–	–	–	39.13	99.54	72.74	110.39	0.981
599.2	3.86	10.39	ND	ND	ND	72.40	0.876	3.24	0.006	–	–	–	–	–	49.06	107.67	73.29	111.59	0.988
Extracted coal (2 °C/h)																			
335.8	0.72	59.64	31.35	1.351	1.260	0.11	0.031	0.12	0.012	0.14	0.12	0.08	–	–	–	29.74	0.16	0.20	0.710
359.8	0.86	56.56	42.96	2.326	1.756	2.23	1.259	1.12	0.662	2.30	9.63	7.23	1.44	0.46	0.08	42.16	4.34	4.89	0.513
384.4[a]	1.08	47.50	49.47	4.841	4.539	6.99	3.888	1.59	2.041	5.08	31.27	31.49	8.38	4.04	2.12	67.64	13.68	15.33	0.511
407.8	1.35	45.50	36.92	3.258	7.772	13.32	6.128	1.69	3.008	6.86	32.77	44.85	5.84	4.42	1.10	62.53	23.34	27.44	0.571
431.9	1.685	41.69	31.66	0.080	9.701	27.67	9.271	3.03	3.497	12.47	34.59	39.60	3.30	2.68	1.82	73.33	41.26	52.24	0.671
432.5[a]	1.694	45.26	26.51	0.085	7.391	27.65	8.893	2.14	3.054	8.49	25.99	30.11	2.16	2.08	6.71	84.28	40.21	51.56	0.688
455.8	2.08	37.57	30.88	–	5.307	33.12	7.473	2.22	1.601	5.19	14.54	6.65	0.27	0.13	4.55	70.48	42.42	57.81	0.781
468.6[a]	2.31	37.22	32.91	–	4.306	48.32	6.204	2.46	0.476	2.15	3.72	0.95	–	–	12.82	89.79	55.05	79.34	0.878
479.8	2.52	32.64	24.42	–	4.252	51.90	4.759	2.86	0.180	5.97	0.57	–	–	–	11.07	82.83	56.85	83.46	0.913
480.7[a]	2.53	34.98	21.73	–	3.762	55.50	3.786	3.65	0.114	8.47	–	–	–	–	16.88	90.44	59.41	88.15	0.934
492.7[a]	2.76	32.57	14.74	–	3.037	62.39	2.610	2.75	0.045	–	–	–	–	–	20.94	96.77	65.05	97.69	0.959
503.8	2.98	28.41	ND	ND	ND	59.13	2.022	1.91	0.031	–	–	–	–	–	23.29	82.54	61.19	92.22	0.966
504.8[a]	3.01	29.56	ND	ND	ND	66.52	1.736	1.73	0.069	–	–	–	–	–	25.65	92.55	68.33	103.32	0.974
516.7[a]	3.24	27.58	ND	ND	ND	70.35	1.361	1.78	0.046	–	–	–	–	–	28.22	96.73	71.76	108.87	0.980
527.8	3.45	23.00	ND	ND	ND	63.33	0.835	1.15	0.029	––	–	–	–	–	33.44	83.90	64.19	97.67	0.987
551.8	3.86	19.87	ND	ND	ND	73.21	0.482	0.95	0.005	–	–	–	–	–	44.57	97.60	73.69	112.50	0.993
575.8	4.18	14.74	ND	ND	ND	86.06	0.386	12.84	–	–	–	–	–	–	54.38	126.10	86.46	132.11	0.995
599.8	4.44	10.69	ND	ND	ND	86.48	0.237	0.00	–	–	–	–	–	–	65.06	144.87	86.72	132.62	0.997
Coal (20 °C/h)																			
335.6	0.57	49.44	23.46	0.695	1.322	0.23	0.042	0.54	0.014	0.36	0.28	0.07	0.03	0.02	0.04	20.97	0.29	0.39	0.789
359.3	0.67	45.54	39.53	1.404	2.353	0.49	0.178	0.76	0.076	0.92	1.41	0.45	0.09	0.00	0.25	28.23	0.76	0.95	0.641
383.7	0.79	41.55	52.95	2.811	3.406	2.12	1.076	2.40	0.481	4.60	5.86	3.87	0.75	0.00	1.09	40.65	3.79	4.44	0.560
407.3	0.95	38.15	54.78	5.077	4.323	4.41	2.618	5.47	1.281	17.54	14.51	14.12	2.23	1.05	4.57	49.09	8.66	9.76	0.510
420.2[a]	1.06	40.13	56.00	5.159	5.012	7.53	3.998	4.51	1.963	13.40	32.17	27.28	10.35	3.58	4.49	52.34	14.25	16.21	0.529
432.2[a]	1.19	37.64	49.87	5.447	6.914	11.38	5.916	7.36	2.793	23.03	37.97	35.20	8.96	3.51	5.98	66.49	20.98	24.18	0.543
444.2[a]	1.33	36.26	38.67	4.129	7.116	14.44	6.872	7.05	3.211	23.30	47.04	44.86	11.29	4.60	6.79	67.08	25.63	29.97	0.563
455.2	1.46	31.25	31.68	1.326	10.491	18.90	7.529	5.57	2.858	14.53	40.87	35.36	6.06	3.03	7.17	56.69	30.17	37.05	0.627
468.1[a]	1.63	28.34	26.81	0.560	9.479	24.83	8.975	6.39	3.636	19.75	56.28	48.05	10.78	4.62	10.65	75.37	38.67	47.89	0.642
479.4	1.79	27.93	22.58	–	9.386	30.69	7.592	4.57	1.495	8.56	11.19	5.43	–	–	8.66	62.99	39.96	54.10	0.768
494.3[a]	2.03	28.35	19.28	–	9.872	38.97	9.394	13.52	1.968	19.74	21.10	8.11	0.65	0.25	13.76	82.36	50.66	68.59	0.769
504.5[a]	2.20	26.76	ND	ND	ND	43.13	7.308	11.54	1.942	9.43	35.32	14.07	–	–	16.59	72.57	52.89	73.31	0.815
516.0[a]	2.40	23.66	ND	ND	ND	55.40	6.957	7.20	0.396	4.31	1.52	0.45	–	–	21.94	91.95	62.78	90.75	0.882

527.9[a]	2.61	22.35	ND	ND	ND	61.81	4.653	14.29	0.140	–	–	–	–	–	26.64	96.59	66.62	98.53	0.928
527.9[a]	2.61	21.90	ND	ND	ND	60.09	4.714	18.96	0.175	–	–	–	–	–	25.03	94.99	65.00	95.98	0.924
551.5	3.05	17.36	ND	ND	ND	73.86	1.863	4.21	0.015	–	–	–	–	–	37.18	89.32	75.75	114.64	0.975
575.8[a]	3.49	14.72	ND	ND	ND	79.44	0.863	2.97	0.005	–	–	–	–	–	59.27	104.75	80.31	122.35	0.989
599.2	3.86	10.52	ND	ND	ND	78.70	0.752	2.65	0.005	–	–	–	–	–	52.82	106.07	79.46	121.13	0.990
Coal (2 °C/h)																			
335.8	0.72	48.82	48.75	1.803	2.555	0.68	0.304	0.50	0.158	0.46	2.24	0.82	0.19	0.04	0.14	30.83	1.17	1.39	0.577
359.8	0.86	45.58	50.68	4.018	3.692	1.29	0.735	0.33	0.343	1.18	5.34	2.75	0.74	0.14	0.65	39.69	2.46	2.81	0.525
383.8	1.07	41.54	42.13	7.118	7.149	6.38	3.532	1.03	1.546	2.33	27.65	16.51	6.23	1.26	1.00	48.20	11.98	13.73	0.533
407.8	1.35	38.51	25.97	3.460	9.196	15.11	6.088	1.02	2.170	3.72	52.20	27.05	16.58	2.91	2.84	52.93	24.36	29.73	0.620
420.4[a]	1.52	40.28	35.75	1.680	9.461	23.58	8.901	2.01	3.075	6.81	28.65	27.89	3.45	2.26	6.04	76.51	36.18	45.35	0.652
432.5[a]	1.694	38.41	27.34	0.138	8.859	30.19	9.005	3.05	2.371	8.00	30.79	17.11	2.68	1.06	7.25	74.87	42.10	55.13	0.717
444.6[a]	1.89	36.06	21.63	–	8.938	37.27	9.036	2.30	1.735	4.87	24.16	7.93	1.00	0.00	8.85	79.10	48.38	65.56	0.770
455.8	2.08	31.12	17.35	–	7.040	38.06	6.771	1.86	0.728	2.27	8.53	1.37	0.13	0.05	7.40	64.32	45.67	64.27	0.833
468.6[a]	2.31	30.36	15.24	–	5.159	54.85	6.804	3.44	0.379	2.24	1.46	0.38	–	–	14.05	92.59	62.06	89.77	0.884
479.8	2.52	27.84	13.76	–	3.267	53.66	3.274	2.58	0.053	–	–	–	–	–	14.02	75.19	56.99	84.87	0.942
480.7[a]	2.53	30.18	15.67	–	4.374	60.60	3.501	4.23	0.087	14.54	–	–	–	–	16.77	84.94	64.21	95.71	0.944
492.7[a]	2.76	28.31	16.98	–	2.665	67.38	2.252	2.41	0.026	–	–	–	–	–	20.95	92.50	69.66	105.03	0.967
504.8[a]	3.01	25.49	ND	ND	ND	70.56	1.360	1.21	0.014	–	–	–	–	–	23.72	96.56	71.94	109.17	0.981
516.7[a]	3.24	24.52	ND	ND	ND	80.64	1.083	1.30	0.011	–	–	–	–	–	34.06	111.63	81.74	124.37	0.987
528.7[a]	3.47	22.35	ND	ND	ND	77.57	0.848	1.43	0.007	–	–	–	–	–	30.71	109.01	78.43	119.48	0.989
551.8	3.86	17.70	ND	ND	ND	82.24	0.430	24.24	–	–	–	–	–	–	49.52	112.81	82.70	126.31	0.995
575.8	4.18	13.68	ND	ND	ND	87.21	0.305	2.46	–	–	–	–	–	–	49.91	120.57	87.52	133.79	0.996
599.8	4.44	10.17	ND	ND	ND	92.74	0.223	–	–	–	–	–	–	–	55.12	154.15	92.96	142.19	0.998
Bitumen rich coal (20 °C/h)																			
335.6	0.57	40.00	69.00	3.176	6.249	0.33	0.107	1.09	0.080	1.79	1.75	1.00	0.35	0.08	0.05	17.49	0.56	0.66	0.601
359.3	0.67	37.50	102.7	3.566	5.741	0.56	0.229	1.02	0.156	2.37	2.37	1.39	0.27	0.06	0.61	26.96	0.99	1.15	0.565
383.7	0.79	34.13	100.5	5.601	7.737	2.31	1.268	3.61	0.875	10.83	13.01	12.23	2.89	1.33	0.99	34.96	4.76	5.18	0.485
408.2[a]	0.96	34.33	92.05	6.243	ND	5.15	3.024	1.30	1.892	15.98	28.85	25.75	7.28	2.66	3.24	17.30	10.73	11.68	0.480
432.2[a]	1.19	31.37	59.61	8.478	10.812	12.06	6.565	7.47	4.020	28.68	60.06	68.06	18.39	8.46	6.38	13.89	24.23	26.73	0.498
444.2[a]	1.33	29.88	61.91	5.985	9.418	14.97	7.354	7.48	4.304	27.91	77.14	84.55	30.29	14.35	7.45	65.68	28.73	32.18	0.521
455.2	1.46	25.99	50.40	2.456	16.642	23.32	11.375	12.50	7.379	66.19	110.87	175.70	0.46	32.34	9.72	65.34	45.35	50.48	0.514
468.1[a]	1.63	27.14	56.37	0.887	16.388	25.62	10.860	25.50	5.788	107.14	88.11	105.72	21.30	12.63	9.51	58.46	44.67	52.33	0.573
479.4	1.79	23.43	57.62	–	17.465	33.39	10.966	7.65	4.586	26.61	52.11	44.96	2.22	1.27	9.79	72.21	49.98	63.08	0.668
494.3[a]	2.03	23.36	38.10	–	13.625	41.15	11.907	8.21	4.638	21.61	86.56	59.43	6.12	3.14	15.04	59.84	59.27	75.98	0.694
503.4	2.18	21.06	ND	ND	ND	44.44	9.792	11.71	2.122	18.64	18.71	3.74	0.20	0.14	16.86	73.21	56.61	77.34	0.785
516.0[a]	2.40	20.39	ND	ND	ND	58.51	9.892	10.97	1.071	10.22	6.73	1.03	0.15	0.13	23.99	65.98	69.57	98.31	0.841
527.6	2.60	18.52	ND	ND	ND	56.73	6.732	17.55	0.478	8.10	1.86	0.28	–	–	24.93	83.59	63.99	92.66	0.887
551.5	3.05	15.93	ND	ND	ND	69.23	3.616	7.03	0.052	–	–	–	–	–	34.95	70.53	72.91	109.00	0.950
551.9[a]	3.06	16.37	ND	ND	ND	77.52	3.157	7.16	0.037	–	–	–	–	–	42.23	77.05	80.72	121.31	0.960
575.3	3.48	12.85	ND	ND	ND	75.87	1.862	4.71	0.016	–	–	–	–	–	41.44	88.61	77.75	117.70	0.976
599.2	3.86	10.26	ND	ND	ND	82.97	1.021	3.49	0.006	–	–	–	–	–	52.27	85.92	84.00	127.89	0.988
Bitumen rich coal (2 °C/h)																			
335.8	0.72	40.10	76.06	3.273	5.169	1.17	0.482	0.67	0.359	2.12	5.16	4.50	0.45	6.86	0.56	24.02	2.18	2.45	0.535
359.8	0.86	37.63	81.58	6.987	8.851	3.15	2.003	1.69	1.530	5.40	22.53	23.78	5.18	2.58	0.66	43.25	7.23	7.54	0.436
383.8	1.07	34.96	61.50	9.624	10.966	6.33	3.672	1.31	2.429	5.28	33.40	40.04	8.88	4.99	1.17	43.62	13.31	14.41	0.476
407.8	1.35	32.31	43.64	7.122	15.025	15.35	7.794	3.81	4.950	16.44	69.50	105.57	20.13	16.59	3.27	54.45	30.23	33.51	0.508
420.4[a]	1.52	32.91	50.44	4.299	19.099	23.60	10.345	2.82	5.503	14.67	66.51	86.38	12.06	9.59	6.39	75.25	41.21	48.38	0.573
431.9	1.685	29.18	44.55	0.394	14.133	28.75	11.472	5.76	6.035	33.24	77.41	111.00	11.31	11.95	6.48	62.04	48.42	57.66	0.594
432.5[a]	1.694	31.81	37.72	0.405	17.874	32.55	12.270	6.36	5.463	27.59	58.10	68.54	6.24	5.41	8.04	64.31	51.70	63.50	0.630
444.6[a]	1.89	28.65	42.93	–	17.133	39.03	12.115	3.05	4.090	11.11	43.45	31.63	2.19	1.35	9.92	79.54	56.04	72.28	0.697
455.8	2.08	26.64	31.16	–	15.693	37.60	10.900	13.88	3.932	45.51	47.21	35.92	1.75	1.04	7.48	78.51	53.35	69.07	0.705
456.6[a]	2.09	28.32	38.73	–	11.562	46.27	10.979	3.72	2.552	7.36	39.93	12.85	1.02	0.26	11.70	73.91	60.36	81.48	0.767
456.6[a]	2.09	28.42	33.69	–	10.988	46.75	11.913	7.49	2.755	14.67	19.52	11.32	–	–	11.44	84.79	61.75	83.00	0.757
468.6[a]	2.31	26.56	36.69	–	8.165	56.43	9.823	3.97	1.053	4.54	4.96	1.47	–	–	14.65	86.47	67.37	95.04	0.837
479.8	2.52	23.56	28.01	–	5.725	57.03	6.701	1.24	0.422	2.45	4.00	1.37	–	–	19.58	65.46	64.22	93.07	0.888
480.7[a]	2.53	25.5	26.27	–	5.696	65.09	6.052	3.26	0.198	–	0.58	0.23	–	–	17.76	74.25	71.35	104.73	0.912

(*continued on next page*)

Table 2 (*continued*)

T (°C)	EASY%R_o	Coal (mg)	Bit	Σn-C_{8+}	Aro	C_1	C_2H_6	C_2H_4 $\times 10^{-3}$	C_3H_8	C_3H_6 $\times 10^{-3}$	i-C_4 $\times 10^{-2}$	n-C_4 $\times 10^{-2}$	i-C_5 $\times 10^{-2}$	n-C_5 $\times 10^{-2}$	H_2 $\times 10^{-2}$	CO_2	ΣC_{1-5}	ΣC_{1-5} (ml/g coal)	$C_1/\sum C_{1-5}$ (wt)
492.7[a]	2.76	24.07	29.88	–	5.013	71.87	4.144	4.87	0.069	–	–	–	–	–	21.08	88.74	76.09	113.48	0.945
503.8	2.98	21.02	ND	ND	ND	68.28	3.097	0.41	0.061	–	–	–	–	–	22.16	91.26	71.44	107.12	0.956
527.8	3.45	18.54	ND	ND	ND	80.00	1.200	3.08	0.020	–	–	–	–	–	31.16	80.91	81.22	123.49	0.985
551.8	3.86	16.18	ND	ND	ND	87.51	0.520	1.39	0.003	–	–	–	–	–	39.84	84.53	88.04	134.43	0.994
576.5[a]	4.19	13.11	ND	ND	ND	100.02	0.339	1.95	0.019	–	0.35	0.21	–	–	82.23	124.72	100.39	153.45	0.996
599.8	4.44	9.81	ND	ND	ND	100.69	0.287	–	–	–	–	–	–	–	48.70	118.83	100.98	154.42	0.997

Bit: bitumen; Aro: aromatics; –: below detection level; ND: not determined.
[a] Data obtained from the second run of pyrolysis experiments.

was performed on a VG Isochrom II interfaced to an HP 5890 GC. The HP 5890 GC was fitted with a Poraplot Q column (30 m × 0.32 mm i.d.). Helium was used as the carrier gas. The column head pressure was 8.5 psi. The GC oven temperature was initially held at 40 °C for 3 min, ramped from 40–180 °C at 20 °C/min, and held at 180 °C for 5 min. The carbon isotopic value of CO_2 reference gas was calibrated by NBS-22 oil as a reference material using elemental analysis (Thermo Quest Flash EA 1112 Series), combined with the isotope ratio mass spectrum (Delta Plus XL). Carbon isotope ratios for individual gaseous hydrocarbons were calculated using CO_2 as a reference gas that was automatically introduced into the IRMS at the beginning and end of each analysis. In addition, a standard mixture of gaseous hydrocarbons (C_1–C_4), with known isotope compositions calibrated by our laboratory, was used daily to test the performance of the instrument. The standard deviation for replicate analyses of this mixture is < 0.3‰ for each compound.

2.4. Liquid hydrocarbon analysis

After analysis for gas components, the capsules that were heated to < 500 °C were cut swiftly into several pieces in a vial, which contained about 3 ml pentane. Two internal standards of deuterated n-C_{22} and n-C_{24}, each ranging from 0.04–0.05 mg were added to each vial. Following five ultrasonic treatments of 5 min per treatment, these vials were allowed to settle for 72 h until the pentane solutions became clear. The pentane solutions (total pentane extracts) in all the vials were directly injected into a HP6890 GC fitted with a 30 m × 0.32 mm i.d. column coated with a 0.25 μm film of HP-5, employing nitrogen as the carrier gas. The oven temperature was programmed as follows: 50 °C for 5 min, from 50–150 °C at 2 °C/min, from 150–290 °C at 4 °C/min and then held at 290 °C for 15 min.

The total pentane extracts of four selected vials were further analyzed using gas chromatography–mass spectrometry (GC–MS) to identify the compounds. The GC–MS analyses were carried out using a Thermal Scientific DSQ II quadrupole mass spectrometer interfaced to a Trace GC ULTRA fitted with a 30 m × 0.25 mm i.d. DB-1MS column with a film thickness of 0.25 μm. Helium was used as the carrier gas. The GC oven temperature was initially held at 50 °C for 5 min, raised from 50–180 °C at 2 °C/min, and from 180–290 °C at 4 °C/min, and then held at 290 °C for 15 min.

After GC and GC–MS analyses, samples in these vials were filtered to separate the pentane solution and the solid residues. The solid residues were Soxhlet extracted with dichloromethane:methanol (93:7 vol:vol) for 72 h. The extracts were combined with the initial pentane soluble fraction to obtain the heavy pyrolysates (bitumen).

2.5. Kinetic modeling of the generation of hydrocarbon gases and vitrinite reflectance

Kinetic parameters were determined for the generation of gaseous hydrocarbons using Kinetics 2000 software developed by Braun and Burnham (1998). At first, we set a range 1×10^9/s–1×10^{13}/s for the A factor, referenced from the previous studies (e.g., Behar et al., 1997; Dieckmann, 2005). After input of the data from the two heating rates, i.e. time, temperature and conversion value for methane generation, a value of the A factor and a discrete distribution of activation energies were obtained. We optimized the kinetic parameters by using a fixed value of A within the range of the three A values obtained from the experiments of extracted coal, coal and bitumen enriched coal. Finally, a fixed frequency factor of 4×10^{11}/s was selected for methane generation in all three experiments, and the activation energies corresponding to this A value were obtained using this software.

Frequency factors of 4×10^{11}/s and 1×10^{14}/s were used for the generation and cracking, respectively, of all the individual wet gases in the three experiments. We first modeled the generation and cracking processes of the individual wet gases separately using the Kinetics 2000 software. The overall process was modeled by the difference between the generation and cracking results.

Sweeney and Burnham (1990) present a vitrinite maturation model to calculate the vitrinite reflectance R_o%, using an Arrhenius first order, parallel reaction approach with a distribution of activation energies (EASY%R_o). This model can be used for time and temperature scales ranging from those in the laboratory to geological processes (Sweeney and Burnham, 1990). However, these authors mention in their paper that the agreement between calculated EASY%R_o and measured R_o% in laboratory experiments with heating times of a few days or less is not adequate. Hill et al. (2003) used EASY%R_o values as a maturity parameter in a series of isothermal oil pyrolysis experiments at temperatures of 350–450 °C and heating times of 1–33.3 days in a confined system (gold capsules). In the present study, two heating rates, i.e., 20 °C/h and 2 °C/h were applied to obtain the kinetic parameters for gas generation and cracking for all three experiments. EASY%R_o was used as a maturity parameter to indicate thermal stress achieved at two heating rates, as in Hill et al. (2003).

3. Results

3.1. Amounts of bitumen, liquid n-alkanes (n-C_{8+}) and aromatic components

The C_6 and C_7 hydrocarbons were heavily evaporated during the analysis of gas components. Therefore, only C_{8+} n-alkanes and aromatic components were measured for the amount of liquid n-alkanes and aromatic components. The amounts of bitumen, liquid n-alkanes (Σn-C_{8+}) and aromatic components are shown in Table 2 and Fig. 1. The gas chromatograms of liquid hydrocarbons for four samples of bitumen rich coal from the 383.8–431.9 °C at 2 °C/h experiment are shown in Fig. 2. The amounts of bitumen, Σn-C_{8+} and aromatic components at first increase and then decrease with temperature and EASY%R_o (Fig. 1). EASY%R_o values for the maximum amounts of bitumen, Σn-C_{8+} and aromatic components are shown in Table 3. The amounts of Σn-C_{8+} are below detection level at EASY%R_o > 1.7 (Tables 2, Figs. 1e and 2).

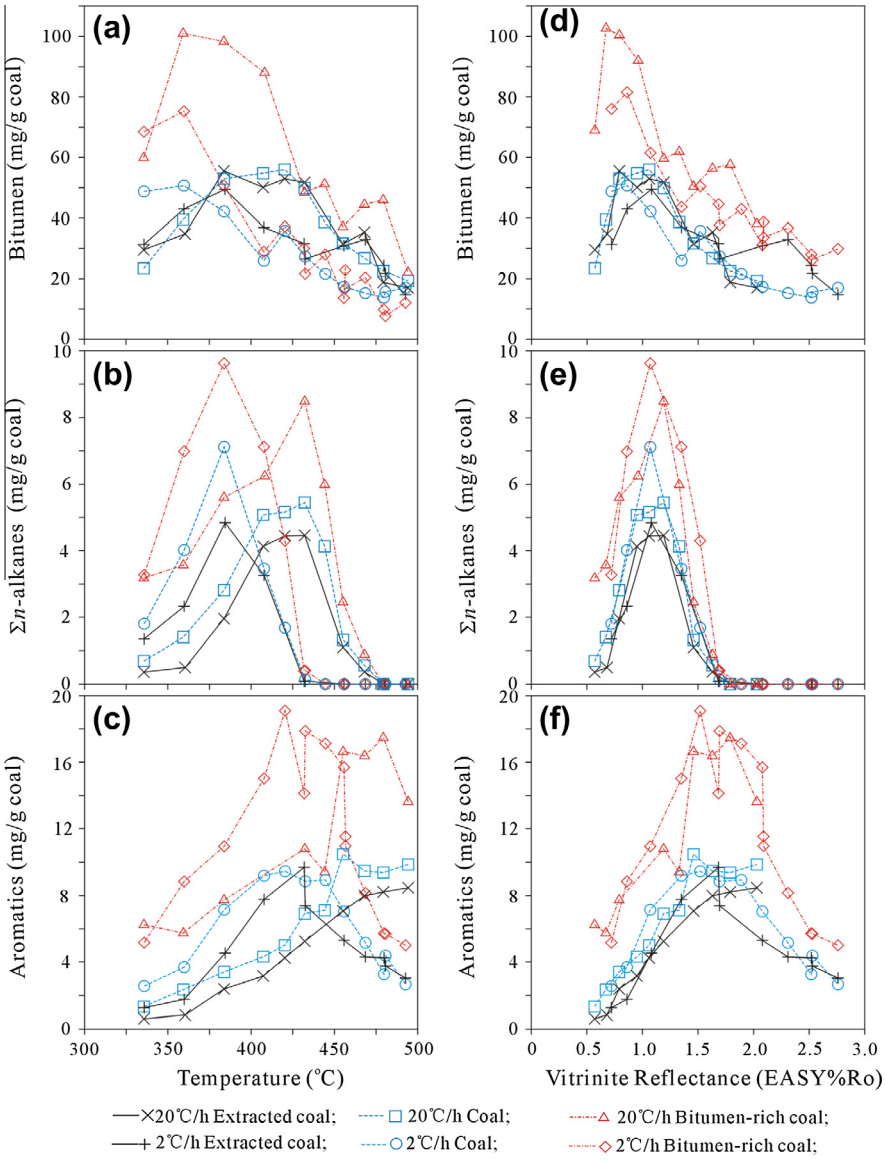

Fig. 1. The amounts of bitumen, Σn-C_{8+} and aromatic components versus temperature and vitrinite reflectance. (a) and (d): amount of bitumen; (b) and (e): amount of Σn-C_{8+}; (c) and (f): amount of aromatics.

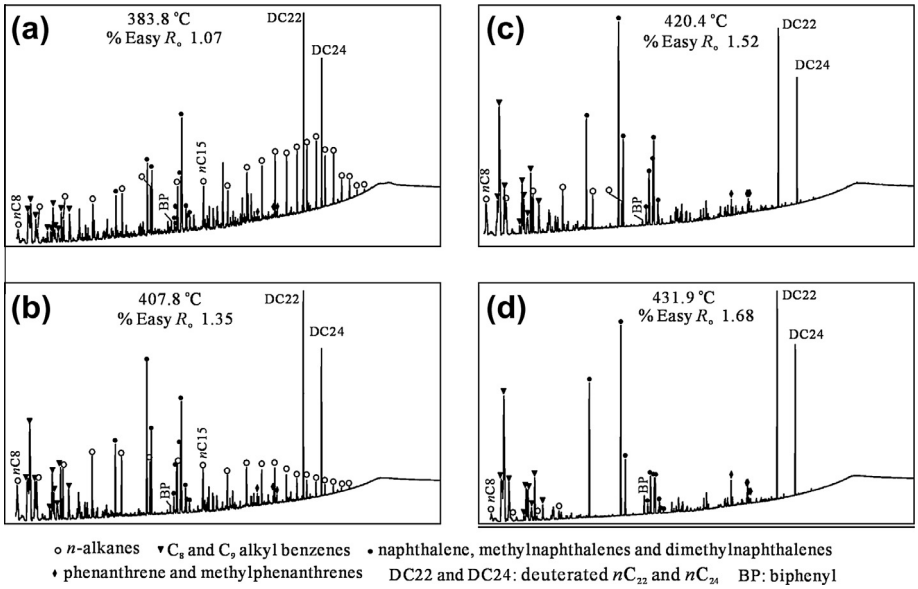

Fig. 2. Gas chromatograms of liquid hydrocarbons from the bitumen rich coal experiment within EASY%R_o 1.07–1.68 at a heating rate 2 °C/h.

Table 3
EASY%R_o values for the maximum amounts of bitumen, ΣnC_{8+}, aromatic components and wet hydrocarbon gases, minimum $C_1/\Sigma C_{1-5}$ and methane $\delta^{13}C$ ratios and the conversion 10% of methane generation.

	Bit	ΣnC_{8+}	Aro	C1	C2	C3	C4	C5	ΣC_{2-5}	$C_1/\Sigma C_{1-5}$	$\delta^{13}C_1$
Extracted coal (20 °C/h)	0.79	1.19	2.03	1.15	2.02	1.63	1.63	1.63	1.63	0.95	0.95
Extracted coal (2 °C/h)	1.08	1.08	1.68	1.21	1.68	1.68	1.35	1.08	1.68	1.08	1.08
Coal (20 °C/h)	1.06	1.19	1.46	1.15	2.02	1.63	1.63	1.33	1.63	0.95	1.19
Coal (2 °C/h)	0.86	1.07	1.52	1.21	1.88	1.52	1.35	1.35	1.52	0.86	1.07
Coal + bitumen (20 °C/h)	0.67	1.19	1.79	1.17	2.02	1.46	1.46	1.46	1.46	0.96	0.95
Coal + bitumen (2 °C/h)	0.86	1.07	1.52	1.24	1.69	1.52	1.68	1.35	1.68	0.86	1.07
Oil (20 °C/h)[a]				1.62	2.60	1.98	1.80	1.62	1.80	1.46	1.47
Oil (2 °C/h)[a]				1.75	2.54	2.10	1.89	1.69	2.10	1.52	1.71
Oil + pyrobitumen (20 °C/h)[a]				1.50	2.18	1.80	1.62	1.46	1.80	1.46	
Oil + pyrobitumen (2 °C/h)[a]				1.68	2.32	1.89	1.89	1.69	1.89	1.52	

Bit: bitumen; Aro: aromatic components; $\delta^{13}C_1$: methane $\delta^{13}C$ values.
[a] Data from Pan et al. (2010, 2012).

The gross composition of the bitumen fraction extracted from the unheated coal is 11.4% saturates, 19.2% aromatics, 23.7% resins and 45.7% asphaltenes. The bitumen fractions obtained after pyrolysis were not analyzed for gross composition due to low amounts.

3.2. Amounts of gas components

3.2.1. Methane

The amounts and ratios of gas components are shown in Table 2. For all three sets of experiments, the amounts of methane increase consistently with temperature and EASY%R_o. At the highest temperature of about 600 °C, the amounts of methane are 72.40, 78.70 and 82.97 mg/g of coal at a heating rate 20 °C/h, and 86.48, 92.74 and 100.69 mg/g of coal at a heating rate 2 °C/h for the experiments on extracted coal, coal and bitumen rich coal, respectively (Table 2).

3.2.2. Ethane, propane, butanes and pentanes

The amounts of ethane, propane, butane, pentane and the total of these gases (ΣC_{2-5}) at first increase to maximum values and then decrease with temperature and EASY%R_o at both heating rates in all three sets of experiments (Table 2). EASY%R_o values for the maximum amounts of these components are shown in Table 3.

3.2.3. Total gaseous hydrocarbons (ΣC_{1-5})

The amounts of total gaseous hydrocarbons increase consistently with temperature and EASY%R_o for all three sets of experiments (Table 2). The maximum amounts are 73.29, 79.46 and 84.00 mg/g of coal at a heating rate of 20 °C/h, and 86.72, 92.96 and 100.98 mg/g of coal at a heating rate of 2 °C/h for the experiments on extracted coal, coal and bitumen rich coal, respectively (Table 2).

3.2.4. H_2 and CO_2

The amounts of H_2 and CO_2 generally increase with temperature and EASY%R_o at both heating rates for all three sets of experiments (Table 2). There is no clear difference in H_2 yield among these three sets of experiments (Table 2). However, the amount of CO_2 is lower for the experiment on bitumen rich coal than the other two sets of experiments under the same experimental conditions (Table 2).

3.3. Ratio $C_1/\Sigma C_{1-5}$

For all three sets of experiments, the $C_1/\Sigma C_{1-5}$ ratio at first decreases and then increases with temperature and EASY%R_o (Table 2). The minimum values are 0.512, 0.510 and 0.480 at a heating rate of 20 °C/h, and 0.511, 0.525 and 0.435 at a heating rate of 2 °C/h for the experiments on extracted coal, coal and bitumen

Table 4
Carbon isotopic compositions ($\delta^{13}C$ ‰ PDB) for gas components.

T	C_1	C_2	C_3	CO_2	T	C_1	C_2	C_3	CO_2	T	C_1	C_2	C_3	CO_2
Extracted coal (20 °C/h)					*Coal (20 °C/h)*					*Bitume rich coal (20 °C/h)*				
335.6	−28.4	−24.3	−24.0	−22.3	335.6	−27.3	−24.7	−24.5	−23.5	335.6	−29.7	−24.7	−22.8	−22.8
360.4	−30.0	−25.7	−26.2	−23.3	359.3	−30.1	−25.8	−24.4	−22.6	359.3	−31.3	−25.2	−24.3	−21.8
383.7	−31.6	−25.6	−23.9	−21.9	383.7	−32.4	−26.4	−24.3	−22.7	383.7	−32.4	−25.7	−23.5	−21.3
407.3	−33.2	−24.9	−23.0	−21.9	407.3	−34.2	−25.7	−23.5	−21.6	407.3	−32.9	−25.8	−25.3	−22.3
431.4	−32.4	−24.9	−23.9	−21.2	431.4	−34.7	−26.0	−23.4	−21.8	431.4	−32.5	−26.0	−24.4	−21.3
455.2	−31.8	−22.5	−21.4	−21.4	455.2	−33.6	−23.4	−21.7	−21.5	455.2	−32.4	−23.7	−23.0	−22.0
479.4	−29.9	−19.8	−17.5	−21.2	479.4	−30.8	−20.1		−21.3	479.4	−31.7	−22.1	−18.6	−21.6
503.4	−28.3	−16.8	−10.9	−21.1	503.4	−28.4	−16.5		−20.2	503.4	−29.8	−17.7	−10.6	−20.2
527.6	−27.1	−11.8		−21.1	527.9	−26.1	−12.6		−20.9	527.6	−28.0	−13.2		−20.6
551.5	−26.0	−7.9		−21.5	551.5	−26.5	−8.3		−21.5	551.5	−26.7	−9.4		−19.2
575.3	−25.8			−21.4	575.8	−23.0			−21.5	575.3	−26.4	−7.6		−19.6
599.2	−24.3			−21.4	599.2	−24.6			−20.8	599.2	−25.9			−21.6
Extracted coal (2 °C/h)					*Coal (2 °C/h)*					*Bitumen rich coal (2 °C/h)*				
335.8	−29.7	−25.1	−24.5	−21.8	335.8	−31.1	−26.9	−25.7	−22.2	335.8	−29.6	−25.5		−21.7
359.8	−32.7	−25.1	−22.9	−21.4	359.8	−34.1	−25.7	−23.1	−21.8	359.8	−34.6	−26.5	−23.7	−22.1
384.4	−33.8	−24.8	−23.0	−22.7	383.8	−34.5	−24.2	−21.5	−21.2	383.8	−34.8	−24.4	−22.4	−21.4
407.8	−33.2	−23.1	−21.2	−21.1	407.8	−33.9	−22.6	−20.2	−21.2	407.8	−34.6	−23.4	−22.2	−20.6
431.9	−31.2	−21.7	−18.5	−21.4	432.5	−32.6	−21.9	−19.2	−21.9	431.9	−31.3	−20.6	−18.0	−22.2
455.8	−29.4	−18.5	−13.9	−21.2	455.8	−29.9	−17.9	−12.6	−22.1	456.6	−28.5	−20.3	−14.6	−22.4
479.8	−27.1	−10.9		−20.3	479.8	−27.9	−11.1		−22.3	479.8	−28.3	−13.6		−20.2
503.8	−25.6	−6.7		−20.5	503.8	−26.4	−8.3		−21.5	503.8	−28.1	−8.7		−20.2
527.8	−25.3			−21.3	527.8	−26.0			−21.7	527.8	−26.0			−20.6
551.8	−24.4			−21.0	551.8	−25.4			−22.1	551.8	−25.4			−21.7
575.8	−23.4			−21.6	575.8	−25.0			−23.3	576.5	−23.1			−21.9
599.8	−23.1			−22.1	599.8	−23.4			−20.2	599.8	−24.6			−21.3

rich coal, respectively (Table 2). For the three sets of experiments, this ratio reaches the minimum value in the EASY%R_o range of 0.86–1.08 (Table 3). At high temperature and EASY%R_o, this ratio increases to 1.0 (Table 2).

3.4. Carbon isotope compositions of gas components

Carbon isotope compositions of methane, ethane, propane and CO_2 are shown in Table 4. Methane $\delta^{13}C$ values at first become more negative and then become less negative with increasing temperature and EASY%R_o for all three experiments. The minimum values are −33.2‰, −34.7‰ and −32.9‰ at a heating rate of 20 °C/h, and −33.8‰, −34.5‰ and −34.8‰ at a heating rate of 2 °C/h for the experiments on extracted coal, coal and bitumen rich coal, respectively (Table 4). For the three sets of experiments, methane $\delta^{13}C$ value reaches the lowest point within the EASY%R_o range of 0.95–1.19 (Table 3).

The $\delta^{13}C$ values of ethane and propane became less negative with increasing temperature for all three experiments. They are generally similar at the same temperature among the three experiments. The reversal for the $\delta^{13}C$ values of ethane and propane is minor or negligible with temperature or EASY%R_o (Table 4).

The $\delta^{13}C$ values of CO_2 for all three sets of experiments are in the range −19.2‰ to −23.5‰, mostly −21.0‰ to −22.0‰. They are very similar among the three experiments and do not show clear trends with temperature or EASY%R_o (Table 4).

4. Discussion

4.1. Mass balance

4.1.1. Bitumen

For the experiment on extracted coal, all bitumen is newly generated. The other two experiments include the initial and newly generated bitumen. At lower maturity (EASY%R_o < 1.0), the bitumen yield from the bitumen rich coal experiment could be the initial value (80.9 mg/g coal) plus the yield from the extracted coal experiment if we suppose that the yield of the newly generated bitumen is the same between these two experiments and that the initial bitumen remains unchanged. However, the yields of bitumen from the experiment on bitumen rich coal at the starting temperature of 336 °C are substantially lower than the sum and even lower than the initial value. The yields of bitumen for bitumen rich coal remain substantially lower than the sum from the starting temperature to those for EASY%R_o of about 1.0 (Table 2, Fig. 1a and d). Furthermore, they decrease rapidly from maximum values at EASY%R_o from 0.67–1.19 at a heating rate of 20 °C/h and 0.86–1.07 at a heating rate of 2 °C/h (Table 2, Fig. 1c). This result suggests that for the bitumen rich coal experiment from the starting temperature to the temperature for EASY%R_o 1.0, bitumen generation was suppressed and/or the initial and newly generated bitumen were partially incorporated into the solid organic residue, as suggested by previous studies (Dieckmann et al., 2006; Erdmann and Horsfield, 2006).

4.1.2. Liquid n-alkanes (n-C_{8+})

The bitumen rich coal contains an initial amount of saturated components of 9.14 mg/g of coal. The difference in the yield of total Σn-C_{8+} is 2.82 mg/g of coal between the two experiments of extracted coal and bitumen rich coal for the starting temperature (336 °C) at a heating rate of 20 °C/h (Table 2). The differences of the maximum yield of Σn-C_{8+} between these two experiments are 4.02 mg/g of coal with EASY%R_o 1.19 at a heating rate 20 °C/h and 4.78 mg/g of coal with EASY%R_o 1.08 at a heating rate 2 °C/h. The differences in the yield of Σn-C_{8+} increase from the starting temperature to the temperatures of maximum yield. This result can be mainly ascribed to cracking of the initial bitumen, especially the aromatic and polar components. It can be deduced that only a minor part of these initial bitumen components cracked, resulting in the formation of 1.20–1.96 mg/g coal of Σn-C_{8+} prior to EASY%R_o of 1.19, assuming that the yields of Σn-C_{8+} from kerogen cracking are the same for these two experiments.

Dieckmann et al. (2000, 2004) documented the heating rate dependence for oil and gas compositions in laboratory pyrolysis. For all three experiments, the maximum yields of bitumen are

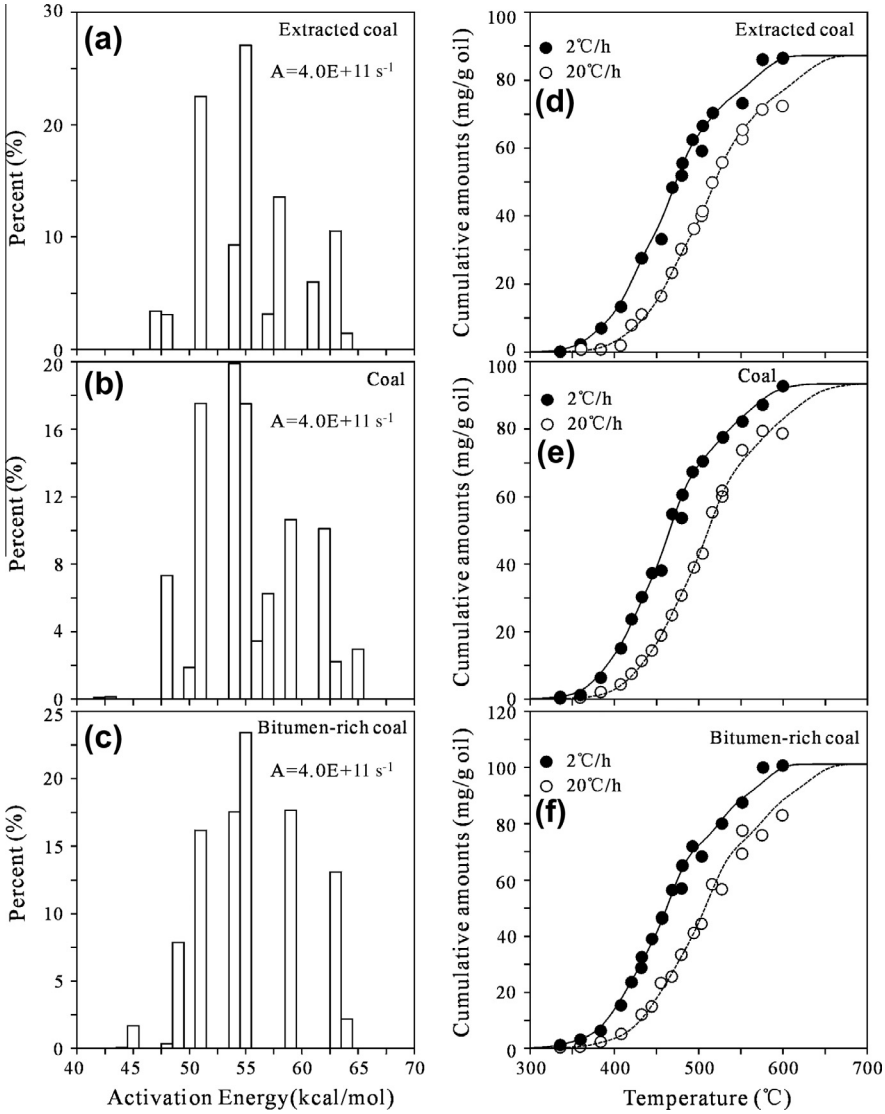

Fig. 3. Activation energy distributions and frequency factors of methane generation (left), and the fit of calculated cumulative amounts of methane with measured results (right).

relatively higher at 20 °C/h than at 2 °C/h, while the maximum yields of Σn-C_{8+} are opposite (Table 2, Fig. 1), indicating a heating rate dependence. This result is consistent with the study of Dieckmann et al. (2000).

4.1.3. Wet hydrocarbon gases (C_2–C_5)

The maximum yield of ethane is 20–25% higher in the bitumen rich coal than the extracted coal and coal experiments, while the maximum yields of C_3, C_4 and C_5 in the former are double or triple those in the latter (Table 2). This result demonstrates that the initial bitumen from bitumen rich coal substantially increased the generation of these wet gases. For the present experiments, the generated gases included both primary and secondary components. The primary gases were generated directly from macromolecular precursors (kerogen, resins and asphaltenes) while the secondary gases were generated from oil or liquid hydrocarbons (e.g., Behar et al., 1992; Prinzhofer and Huc, 1995; Erdmann and Horsfield, 2006). As indicated by the yields of Σn-C_{8+}, the yields of liquid hydrocarbons are substantially higher in the bitumen rich coal than in the extracted coal and coal experiments. The higher yields of wet gases in the former can be mainly ascribed to secondary cracking of liquid hydrocarbons. In other words, the wet gases mainly originate by secondary cracking. It can be further deduced that in the bitumen rich coal experiment the proportions of gas from secondary cracking increase with carbon number because the yield differences for the wet gases are increasingly greater with carbon number between the bitumen rich coal and the other two coals.

The maximum ethane yields are similar at both heating rates and do not show consistent trends with heating rate for the three experiments (Table 2). For propane to pentanes, the measured maximum yields between the two heating rates differ significantly (Table 2, Fig. 3). Both the maximum yields of propane and butanes increase with heating rate for the three experiments, in contrast to Dieckmann et al. (2004). The maximum yields of pentanes vary with heating rate for the three experiments. The discrepancy of the measured maximum yields for propane to pentanes between the two heating rates in the present study can be mainly ascribed to the relatively low yields and few data points.

4.1.4. Methane

The yields of methane are about 13, 15 and 16 mg/g of coal at EASY%R_o 1.35 and 41, 43 and 48 mg/g of coal at EASY%R_o 2.20 for the experiments of extracted coal, coal and bitumen rich coal,

respectively (Table 2, Fig. 3i). At EASY%R_o 2.20, the yields of Σn-C_{8+} are below the detection level, while those of aromatic components are decreasing and lower than 10 mg/g of coal (Table 2, Fig. 1). In addition, the yields of the total wet gases (ΣC_{2-5}) are decreasing and lower than 9.56, 9.76 and 12.00 mg/g coal in the extracted coal, coal and bitumen rich coal experiments, respectively (Table 2). Therefore, nearly half of the maximum yield of methane was generated at EASY%R_o > 2.2 from kerogen. The differences in methane yields among the three experiments at same temperature are relatively minor at EASY%R_o < 2.2, but greater with temperature at EASY%R_o > 2.2 (Table 2). This result demonstrates that the solid organic residue always retained more hydrogen and higher hydrocarbon generative potential at the postmature stage in the bitumen rich coal than the extracted coal and coal experiments, consistent with previous studies (Dieckmann et al., 2006; Erdmann and Horsfield, 2006).

4.1.5. Ratio $C_1/\Sigma C_{1-5}$

For all three experiments, the decrease in $C_1/\Sigma C_{1-5}$ to minimum values closely corresponds to the increase in yields of bitumen and Σn-C_{8+} to maximum values with temperature and EASY%R_o (Tables 2 and 3). This phenomenon was also observed in experimental studies on type I and II kerogens (e.g., Lorant et al., 1998; Pan et al., 2008). One possible interpretation is that the initial gases were mainly generated from reactive moieties (mainly methyl groups) with labile bonds attached to kerogen or polar components, while the later gases were partially generated from alkyl groups attached to aromatic rings. The initial gases contained relatively more methane than later gases. The ratio of gases from the cracking of stable bonds to those of labile bonds increases with temperature and maturity. EASY%R_o values for the minimum $C_1/\Sigma C_{1-5}$ are significantly lower than those for the highest ΣC_{2-5} yields, i.e. about 1.0 and 1.5, respectively (Table 3). It appears that $C_1/\Sigma C_{1-5}$ is simply controlled by the amount of Σn-C_{8+} relative to kerogen in all the three experiments, although the actual mechanism is unknown. This ratio is lower in the bitumen rich coal than the extracted coal and coal experiments because of higher yields of Σn-C_{8+} for the former than the latter, especially at EASY%R_o < 2.0 (Table 2).

Pan et al. (2012) demonstrated that pyrobitumen significantly accelerated the generation of methane relative to wet gases and therefore $C_1/\Sigma C_{1-5}$ was higher in the pyrolysis experiment of oil plus pyrobitumen than oil alone. Minimum $C_1/\Sigma C_{1-5}$ values occur at EASY%R_o 1.46–1.52 in their study (Table 3). This reversal might be related to the compositional variation of residual oil.

4.2. Stabilities of alkanes and wet gases

There is considerable overlap between the generation and cracking of the liquid *n*-alkanes and wet gases (e.g., Dieckmann et al., 2000; Hill et al., 2003; Pan et al., 2012). When the yields of liquid *n*-alkanes and wet gases reach maximum values, the generation rates equal the removal rates by cracking of these components. The variation of the yield of Σn-C_{8+} demonstrates that significant cracking of these compounds began at least at EASY%R_o 1.0 in all three experiments, which is substantially lower than that in oil pyrolysis experiments (e.g., Horsfield et al., 1992; Hill et al., 2003; Pan et al., 2010, 2012). However, this result is consistent with the conventional observation that the residual yields of hydrocarbons in source rocks generally reach the highest values at R_o% around 1.0 based on field data (e.g., Tissot and Welte, 1984). In sedimentary basins, the residual hydrocarbon yield from source rock is the overall result of hydrocarbon generation, cracking and expulsion within this rock. Previous studies suggest that a value of 200 mg/g TOC is an approximate minimum initial hydrogen index required for oil expulsion (e.g., Pepper, 1992; Pepper and Dodd, 1995; Pepper and Corvi, 1995). Oil cracking is substantially faster in source rocks than conventional reservoir rocks possibly due to catalysis by kerogen and minerals in source rocks (e.g., Pepper and Dodd, 1995; Schenk et al., 1997; Dieckmann et al., 1998; Hill et al., 2007). Pan et al. (2010) demonstrated that neither montmorillonite nor calcite significantly influence the primary cracking of oil components (C_{6+}) to gaseous hydrocarbons (C_1–C_5). However, they found later that pyrobitumen significantly promotes the generation of methane while both inhibiting the generation and accelerating the cracking of wet gases (Pan et al., 2012).

The values of EASY%R_o for the highest yields of wet gases are significantly lower in all three experiments than in the pyrolysis experiments of oil alone or oil plus pyrobitumen performed by Pan et al. (2012, Table 3), demonstrating that the cracking rates of wet gases are greater in the former versus the latter experiments. The coal, or kerogen, apparently plays an important role in catalyzing the cracking of wet gases, as well as liquid *n*-alkanes.

Activated carbon was found to accelerate the cracking of hydrocarbons in an early study (Greensfelder et al., 1949). Smith et al. (1989) used hydrous pyrolysis experiments to show that brown coal accelerates the transformation of model compounds into *n*-alkanes and transformation rates increase with the ratios of the added coal to model compounds, including long chain *n*-alkyl constituents, such as *n*-alcohol, di-*n*-ketone, di-*n*-ether, *n*-acid and alkyl aromatics. Recently, Alexander et al. (2011) demonstrated that activated carbon and coal substantially accelerate the transformations of 1-octadecene and 2,3,6-trimethyphenol into gaseous and liquid products. They suggested that surface reactions of hydrocarbons on solid carbonaceous material in sediments (e.g., coal, kerogen, pyrobitumen and black carbon) play an important role in the formation of crude oil and natural gas. The results of the present study are consistent with previous studies.

4.3. Kinetic parameters

4.3.1. Kinetic parameters for the generation of methane

Hydrocarbon generation from kerogen is generally described using a set of parallel first order reactions with a single frequency factor and a distribution of activation energies (e.g., Ungerer and Pelet, 1987; Schenk and Horsfield, 1993; Tang et al., 1996; Behar et al., 1997). For coal samples, simplified kinetic models with a single frequency factor are not sufficient to correctly predict hydrocarbon generation under geological conditions (e.g., Dieckmann, 2005). The main purpose for the kinetic modeling in the present study is to characterize the differences in kinetic properties for the generation of gas hydrocarbons among the three experiments of extracted coal, coal and bitumen rich coal. Previous studies demonstrated the compensation effect between the frequency factor (A) and the activation energies for hydrocarbon generation and destruction (e.g., Pelet, 1994; Waples, 2000; Pan et al., 2012). In order to avoid this compensation effect, we used a fixed frequency factor of 4×10^{11}/s for methane generation in all three experiments. This frequency factor is suitable for early methane generation, but lower for late methane generation from coal samples (e.g., Behar et al., 1997; Dieckmann, 2005). The kinetic parameters for the generation of methane are listed in Table 5. The activation energy distributions and the fit of the cumulative amounts of methane calculated from the kinetic parameters and measured from the experiments are shown in Fig. 3.

4.3.2. Kinetic parameters for the generation and cracking of wet gases

Few publications have reported or noted the kinetic parameters for the generation and cracking of wet gases (e.g., Tsang, 1989; Behar et al., 1992; Pepper and Dodd, 1995; McNeil and BeMent, 1996; Lorant et al., 1998; Dieckmann et al., 2004; Shuai et al., 2006), in contrast to the enormous amounts of kinetic data for

Table 5
Kinetic parameters for hydrocarbon gases.

Extracted coal		Coal		Bitumen rich coal	
Ea (kcal/mol)	Fraction (%)	Ea (kcal/mol)	Fraction (%)	Ea (kcal/mol)	Fraction (%)
Methane generation A = 4 × 10^{11} s^{-1}					
47	3.43	42	0.10	44	0.05
48	3.10	43	0.14	45	1.68
51	22.50	48	7.31	48	0.33
54	9.27	50	1.88	49	7.88
55	27.05	51	17.52	51	16.16
57	3.16	54	19.90	54	17.52
58	13.54	55	17.51	55	23.43
61	6.01	56	3.45	59	17.66
63	10.51	57	6.24	63	13.11
64	1.43	59	10.65	64	2.18
		62	10.11		
		63	2.23		
		65	2.97		
Ethane generation Ag = 4 × 10^{11} s^{-1}					
47	8.36	41	0.10	45	6.59
48	39.72	48	56.00	46	3.30
51	50.21	50	1.43	49	49.28
55	1.70	51	42.47	51	37.30
				52	2.19
				56	1.34
Ethane cracking Ac = 1 × 10^{14} s^{-1}					
63	37.12	60	2.80	60	5.00
64	38.78	63	22.28	63	8.58
67	12.84	64	57.18	64	57.69
68	1.91	67	2.43	67	9.88
72	9.35	68	9.49	68	11.60
		73	5.82	71	3.92
				73	3.33
Propane generation Ag = 4 × 10^{11} s^{-1}					
47	3.70	41	0.27	45	6.53
48	75.93	42	0.31	46	5.89
51	20.07	48	66.44	48	22.26
55	0.30	51	23.50	49	36.18
		52	8.33	51	22.50
		55	1.14	52	6.63
Propane cracking Ac = 1 × 10^{14} s^{-1}					
61	38.59	60	88.87	60	47.30
62	58.98	63	9.02	62	18.18
66	1.42	64	2.11	63	34.20
68	1.02			68	0.31
Butane generation Ag = 4 × 10^{11} s^{-1}					
47	0.76	48	50.62	41	0.24
48	48.77	49	28.79	44	2.97
51	47.94	51	8.43	45	0.73
52	0.78	52	11.78	48	54.52
56	1.75	56	0.38	51	40.27
				52	0.41
				55	0.87
Butane cracking Ac = 1 × 10^{14} s^{-1}					
59	56.03	59	82.63	59	48.34
61	30.93	62	17.37	61	13.44
62	11.74			62	38.22
67	1.30				
Pentane generation Ag = 4 × 10^{11} s^{-1}					
48	85.02	48	11.86	45	6.30
49	13.95	49	72.64	46	6.35
54	1.04	51	15.47	49	56.44
		54	0.04	50	30.70
				53	0.21
Pentane cracking Ac = 1 × 10^{14} s^{-1}					
58	0.78	58	77.44	59	82.32
59	90.15	61	14.19	60	16.99
63	7.92	62	8.37	65	0.69
67	1.16				

the generation and cracking of oil components. Pan et al. (2012) determined the kinetic parameters for the generation and cracking of individual wet gases from pyrolysis experiments on oil and oil plus pyrobitumen. However, the amounts of oil relative to solid organic residue were excessive in the previous study (> 50%), unlike the present study (< 5%). Therefore, kinetic properties for

the generation and cracking of wet gas hydrocarbons differ in the previous and present studies.

Dieckmann et al. (2000) evaluated the overlap of primary and secondary reactions of oil components by a combination of closed and open system pyrolysis experiments of marine kerogen. They suggested that the overlap of primary and secondary reactions only affects the overall composition of the C_{6+} fraction in the closed system but not the timing of secondary gas formation. In principle, the extent of overlap for the generation and cracking of individual alkanes increases with carbon number because the cracking temperature decreases with carbon number, especially for light alkanes.

In the present study, we assume that the maximum amount of the individual wet gases represents 95% conversion, and then, the individual wet gases begin to crack. For C_3 to C_5 gases, the measured maximum yields differ significantly between the two heating rates. We used the higher yield results to calculate the kinetic parameters for the generation and cracking of individual wet gases (Table 5). The activation energy distributions and the fit of the cumulative amounts calculated from the kinetic parameters and measured from the experiments for the individual wet gases are shown in Figs. 4–7. The differences in peak or averaged activation energies are only 9–14 kcal/mol between the generation and cracking for wet gases using the different frequency factors. If the same frequency factor is used, i.e., 1×10^{14}/s, for both generation and cracking, the differences in peak or averaged activation energies are only 2–7 kcal/mol between the generation and cracking of these gases.

Pan et al. (2012) demonstrated that the activation energies for the generation and cracking of wet gases decrease with carbon number and are lower in the experiments of oil plus pyrobitumen than oil alone. In the present study, the averaged values of activation energies for the generation of individual wet gases do not vary significantly with carbon number. However, activation energies for cracking of these gases decrease with carbon number, reflecting decreased thermal stabilities of these components with carbon number, consistent with the previous study (Pan et al., 2012).

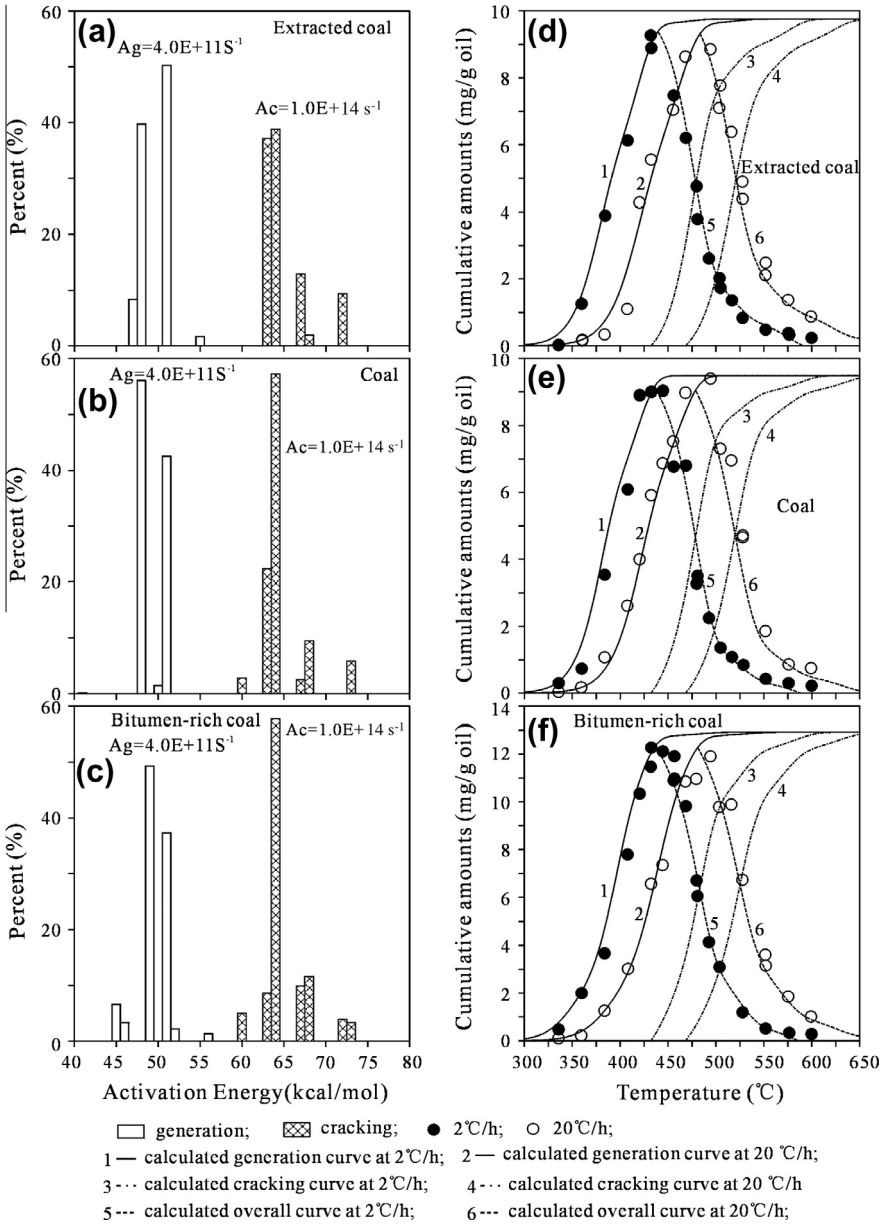

Fig. 4. Activation energy distributions and frequency factors of ethane generation and cracking (left), and the fit of calculated cumulative amounts of ethane with measured results (right).

It can be deduced that primary cracking gas is generated at lower thermal stress than secondary cracking gas, and therefore, activation energies for the generation of primary cracking gas are lower than those of secondary cracking gas from previous studies on kerogen and oil pyrolysis (e.g., Behar et al., 1992; Horsfield et al., 1992; Hill et al., 2003; Erdmann and Horsfield, 2006). The wet gases have higher ratios of the secondary cracking components from liquid hydrocarbons to the primary cracking components from kerogen in the bitumen rich coal experiment compared to the other two experiments. Furthermore, in principle, kerogen catalytic capability likely decreases with oil/kerogen ratio. It might be deduced that activation energies are higher for the generation and cracking of wet gases in the bitumen rich coal experiment than the other two experiments. However, the averaged values of activation energies for both the generation and cracking of individual wet gases are similar and lack consistent trends among the three experiments (Table 5, Figs. 4–7). This result can be interpreted as follows. First, there may be no substantial difference in kinetic properties between the generation of primary and secondary wet gases in the experiments because the stability of oil components is substantially reduced in the presence of excess coal. Second, the oil/kerogen ratio was very low for all three experiments (< 5%). Therefore, the differences for this ratio may not significantly influence the catalytic activity of kerogen.

The activation energies for the generation and cracking of individual wet gases (C_2–C_5) are substantially lower in the three experiments compared with the previous oil and oil plus pyrobitumen pyrolysis experiments (Pan et al., 2012). The averaged activation energies for the generation of these components are about 8–11 kcal/mol lower with frequency factor 4×10^{11}/s and 2–4 kcal/mol lower with frequency factor 1×10^{14}/s in the present experiments compared to the previous oil and oil plus pyrobitumen pyrolysis experiments with frequency factor 1×10^{14}/s. Averaged activation energies for the cracking of these gases are about

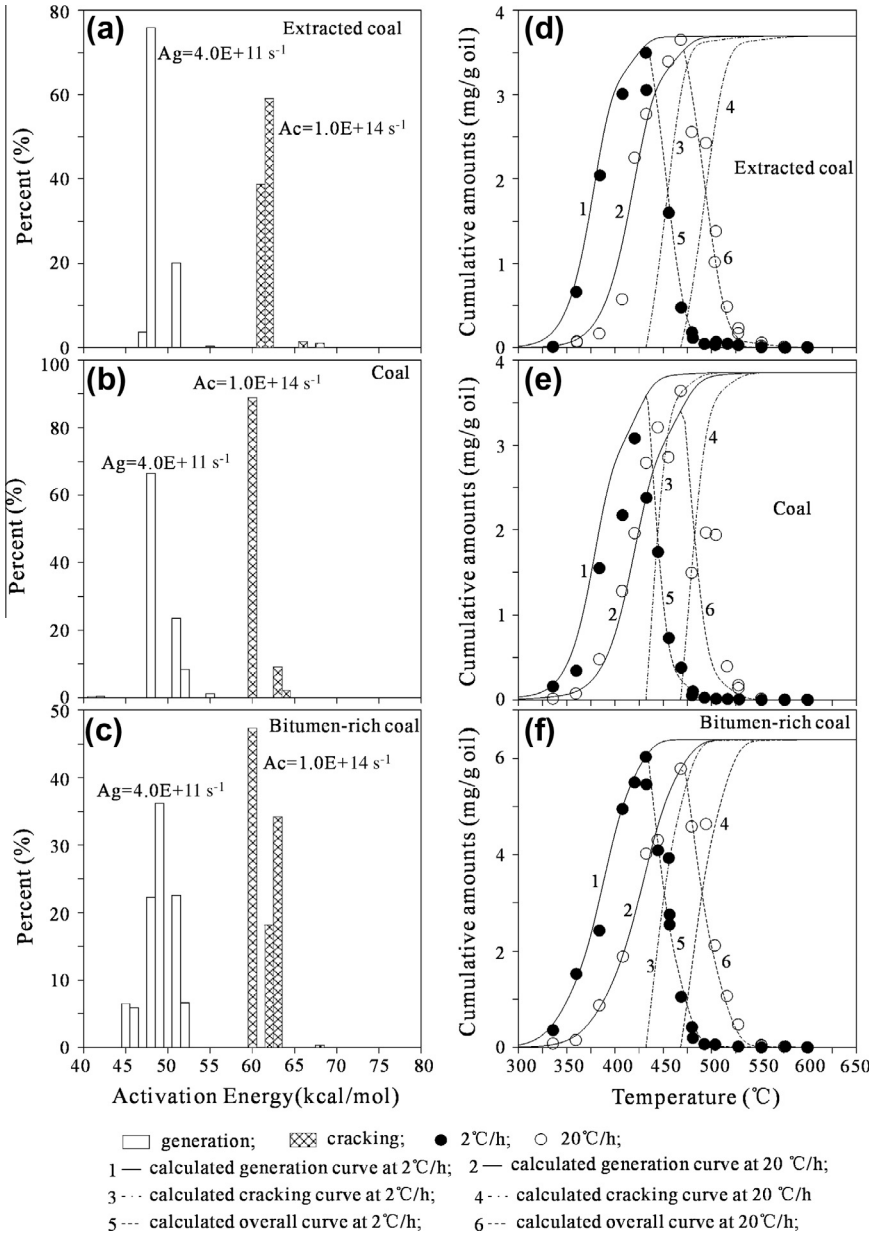

Fig. 5. Activation energy distributions and frequency factors of propane generation and cracking (left), and the fit of calculated cumulative amounts of propane with measured results (right).

5–10 kcal/mol lower with frequency factor 1×10^{14}/s and 2–7 kcal/mol lower with frequency factor 1×10^{15}/s in the present experiments compared to the previous oil and oil plus pyrobitumen pyrolysis experiments with frequency factor 1×10^{15}/s.

4.4. Precursors of hydrocarbon gases implied from carbon isotopes

Previous studies demonstrated that methane $\delta^{13}C$ values at first decrease to a minimum value, and then increase with temperature or R_o% in confined pyrolysis experiments on kerogen and coal samples (Lorant et al., 1998; Tang et al., 2000; Liu et al., 2004; Xiong et al., 2004; Xiao et al., 2005, 2006, 2009; Tian et al., 2012), as observed in the present study (Table 4). Using the method of Tang et al. (2000), this trend for methane $\delta^{13}C$ values can be modeled mathematically (e.g., Xiao et al., 2005, 2006, 2009; Tian et al., 2012). The reversal in methane $\delta^{13}C$ values with temperature and R_o% can be interpreted to be the result of two precursors for methane. First, methane can be generated from methyl groups by cracking labile bonds between carbon and heteroatoms. Second, methane can be generated from methyl or alkyl groups by cracking of C–C bonds. The first precursor is characterized by either heavier initial isotopes (higher $\delta^{13}C$ value; Cramer, 2004) or minor isotope fractionation (lower ΔEa) during methane generation (Tang et al., 2000) or both. In contrast, the second precursor is characterized by either lighter initial isotopes (lower $\delta^{13}C$ value, Cramer, 2004), or major isotope fractionation (higher ΔEa) during methane generation (Tang et al., 2000) or both. The initial methane is largely from the first precursor while later methane is increasingly from the second precursor. At high temperatures or EASY%R_o values in our experiments, the accumulated methane was dominantly from the second precursor with very minor contribution from the first precursor. In addition, during methane generation from the first precursor, no or very little wet gas is generated, while during methane generation from the second precursor, high amounts of

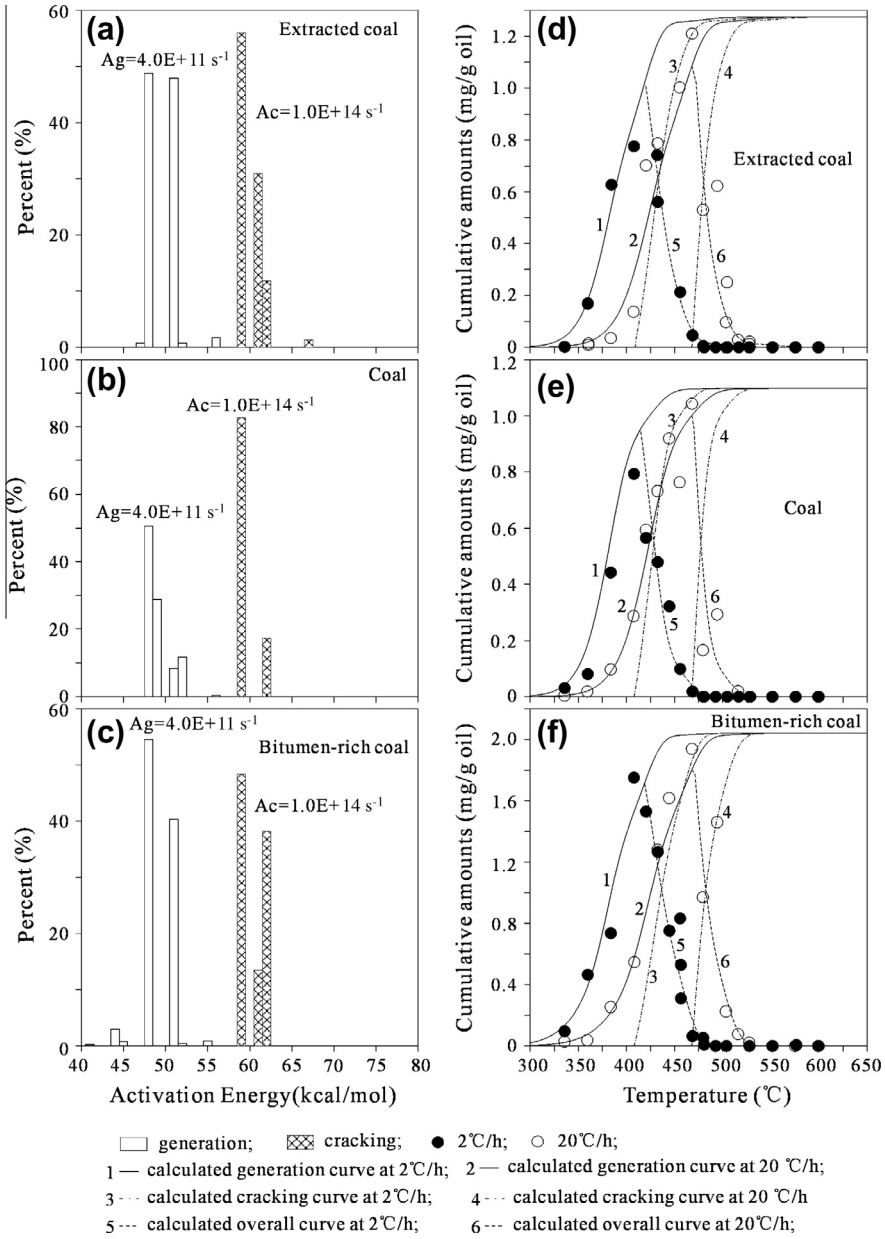

Fig. 6. Activation energy distributions and frequency factors of butane generation and cracking (left), and the fit of calculated cumulative amounts of butane with measured results (right).

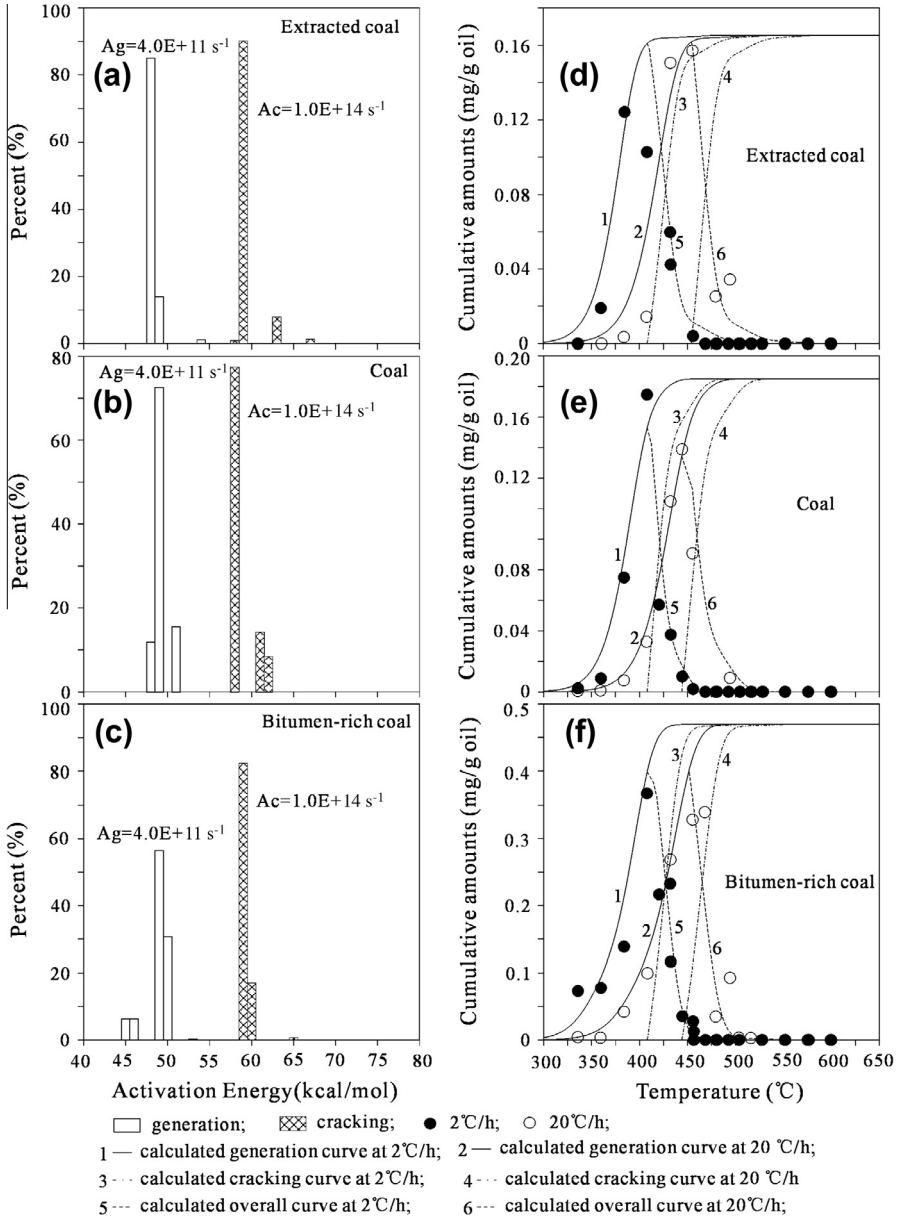

Fig. 7. Activation energy distributions and frequency factors of pentane generation and cracking (left), and the fit of calculated cumulative amounts of pentane with measured results (right).

wet gas were generated, especially at lower temperatures or EASY%R_o < 1.0. Therefore, methane $\delta^{13}C$ values co-varied with the $C_1/\Sigma C_{1-5}$ ratio (Tables 2–4).

Another interesting phenomenon is that methane $\delta^{13}C$ values at the maximum temperature or EASY%R_o are similar to those of initial wet gases, especially C_3, i.e., about −24‰ for all three experiments (Table 4). These $\delta^{13}C$ values are lower (lighter) than the $\delta^{13}C$ value of the initial coal sample, i.e. −22.86‰ (Table 1). This phenomenon was also observed in previous confined pyrolysis studies on type II kerogen (Lorant et al., 1998), purified vitrinite from three different coals (Liu et al., 2004) and asphaltenes separated from crude oil (Tian et al., 2012). This result may indicate that most methane shared a common precursor with wet gases in confined pyrolysis experiments. During confined pyrolysis of kerogen or asphaltenes, the formation of wet gases, especially C_3–C_5, created very minor carbon isotopic fractionation. Therefore, the $\delta^{13}C$ values of the initial wet gases could be very similar to the $\delta^{13}C$ values of the initial precursor and the accumulated methane at the final generation stage. It can be deduced that for all three experiments both methane and wet gases were mainly generated from free alkanes and the alkyl groups bound to macromolecules, including aromatics, resins, asphaltenes and kerogen. As documented earlier, the maximum yields of Σn-C_{8+} are substantially lower than the maximum yields of methane and lower than the maximum yields of ethane (Table 2). This result suggests that the yields of free Σn-C_{8+} only represent a small part of the total mass of the free liquid alkanes and bound alkyl groups. For coal and type III kerogen, only a small part of the bound alkyl groups can be released as liquid alkanes. In addition, the released alkanes can reattach to the kerogen (McNeil and BeMent, 1996; Boreham et al., 1999; Erdmann and Horsfield, 2006). Erdmann and Horsfield (2006) suggested that the recombination reactions of liquid products released from type III kerogen at low levels of maturation result in formation of a thermally stable bitumen, which generates methane at higher maturity. Pan et al. (2012) suggested that some oil and wet gas components were combined into pyrobitumen and

released later, mainly as methane at higher temperatures and maturities during pyrolysis of oil plus pyrobitumen.

According to the reaction model of McNeil and BeMent (1996), the alkyl group cleaves from aromatic rings in the kerogen to form an alkyl radical having one less carbon than the original alkyl group. Within oil generation window, this released radical may capture a hydrogen radical and form an alkane. Within the gas window, this released radical may immediately reattach to aromatic rings in the kerogen. The increase in $\delta^{13}C$ values of wet gases with temperature and EASY%R_o can be interpreted as the result of their cracking, as well as the increase of the $\delta^{13}C$ value of the residual free alkanes and bound alkyl groups due to methane generation.

In summary, methyl groups which form methane can be classified into two types: those attached to the macromolecules by labile bonds, and those attached by more stable C–C bonds. These two types can have different origins. The first type is present in the initial coal while the second type is most likely absent in the initial coal, but forms later from the free and bound alkanes via a reaction mechanism suggested by McNeil and BeMent (1996). At high maturation, the amount of methane formed from the first type of methyl group represents only a minor portion, while that from the second type of methyl group represents the major portion of the total methane yield.

For all three experiments, the $\delta^{13}C$ values of CO_2 vary within −19‰ to −23‰, mostly in the range −20‰ to −22‰, and do not show a clear trend with temperature and maturity, possibly implying that CO_2 formation did not induce significant carbon isotopic fractionation.

4.5. Implications

Coal measures are the most important source rocks for hydrocarbon gases in Chinese gas reservoirs, especially the giant gas fields (e.g., Dai et al., 1997, 2003, 2005, 2008). Several studies of the Kela 2 gas field, the largest in the Tarim Basin, China, demonstrated that hydrocarbon gases in this field were generated from Jurassic coal source rocks at the postmature stage (R_o% > 1.3, Zhao et al., 2002; Liang et al., 2003; Zhao et al., 2005). Hydrocarbon gases in this field have very high $C_1/\Sigma C_{1-5}$ ratios ranging from 0.99–1.0, and heavy carbon isotopic composition, i.e., $\delta^{13}C$ values of methane and ethane in the range −26.2‰ to −28.2‰ and −16.6‰ to −19.4‰, respectively (e.g., Liang et al., 2003; Zhao et al., 2005). In addition, the present maturities of the Jurassic coals in the source kitchen for this gas field are very high with Ro% > 2.0 (Zhao et al., 2002; Liang et al., 2003; Zhao et al., 2005). For the three experiments in the present study, methane yields at EASY%R_o 1.35 and 2.20 are about 15% and 45–47% of the maximum values for the coal samples, respectively. The weights of the total hydrocarbon gases (ΣC_{1-5}) at EASY%R_o 1.35 and 2.20 are 26–30% and 56–62% of the maximum values for the coal samples, respectively. Furthermore, coals having higher initial HI values and hydrogen contents generate higher amounts of bitumen and oils at the maturity of oil generative window. Most bitumen and oils are retained in the coals except that minor excessive oils are expelled from the coals (Pepper, 1992; Sandvik et al., 1992). These coals are more favorable for late methane generation due to the re-incorporation of bitumen and oils into the kerogen, compared with those having lower initial HI values and hydrogen contents. This result is consistent to the previous studies emphasizing the importance of deep methane (Dieckmann et al., 2006; Erdmann and Horsfield, 2006).

The observation that $C_1/\Sigma C_{1-4}$ ratios are substantially higher for hydrocarbon gases in natural reservoirs than those generated in oil and kerogen pyrolysis experiments has been documented in previous studies (e.g. Mango et al., 1994; Mango, 1997, 2001). Transition metal catalysis has been suggested as the formation mechanism for hydrocarbon gases in sedimentary basins based on the results of pyrolysis experiments on artificial samples (e.g., Mango, 1992, 1997, 2001). According to this mechanism, lower activation energies for the cracking of wet gases in the three experiments in this study compared to oil cracking experiments in previous studies may be ascribed to catalysis of transition metals in the coal. However, transition metal catalytic processes have been questioned (e.g., McNeil and BeMent, 1996; Snowdon, 2001; Lewan et al., 2008). In particular, the result of hydrous pyrolysis experiments on source rocks rich in transition metals demonstrates that transition metals have no effect on methane yields (Lewan et al., 2008).

Kerogen and solid organic matter (pyrobitumen) in source and reservoir rocks substantially reduce the stabilities of oil and wet gases, as demonstrated in the present and previous studies (e.g., Alexander et al., 2011; Pan et al., 2012). Due to the catalysis of kerogen, oil cracking occurs at lower thermal stress in source rocks compared to reservoir rocks. In addition, stabilities of oils and wet gases can differ substantially in reservoir rocks in the presence and absence of pyrobitumen. For example, reservoir rocks of gas fields in the Sichuan basin contain abundant of pyrobitumen and very dry hydrocarbon gases with $C_1/\Sigma C_{1-4}$ ratios ranging 0.975–1.0 (e.g., Hao et al., 2008; Liu et al., 2013). In these reservoirs, pyrobitumen accelerated the cracking of oil components and wet gases. In contrast, oil components remain stable in two condensate reservoirs under high temperature (175–200 °C), as reported by McNeil and BeMent (1996), possibly due to the lack of solid organic matter (pyrobitumen) in the reservoir rocks.

5. Summary

For all three experiments, nearly half of the maximum amount of methane was generated from kerogen at EASY%R_o > 2.2. The differences in the methane yields among the three experiments are minor at EASY%R_o < 2.0, but they are increasingly greater with temperature and maturity, indicating the solid residue always retained relatively higher amount of hydrogen and higher hydrocarbon generative potential at postmature stage in the bitumen rich coal compared to the extracted coal and coal experiments. The maximum yields of wet gases are substantially higher for bitumen rich coal than extracted coal and coal. It can be deduced that a larger portion of wet gases were generated from secondary cracking of liquid hydrocarbons in the bitumen rich coal. However, the averaged values of activation energies for both the generation and cracking of individual wet gases are similar and do not show consistent trends among the three experiments with the same frequency factors. For all three experiments, the activation energies for the generation and cracking of wet gases are significantly lower than those in oil pyrolysis experiments with same frequency factors. In addition, lower EASY%R_o values for the maximum yields of total liquid *n*-alkanes for the three experiments compared with oil pyrolysis experiments demonstrates that the stability of these components is greatly reduced in the presence of coal.

Methane $\delta^{13}C$ values correlate positively with $C_1/\Sigma C_{1-5}$ ratios. Methane $\delta^{13}C$ values at the maximum temperature or EASY%R_o are very similar to those of initial wet gases, especially C_3, implying that the major part of methane shared a common precursor with wet gases. Both methane and wet gases were mainly generated from the free and bound alkanes, while methyl groups with labile bonds attached to kerogen in the initial coal samples are minor compared with the free and bound alkanes.

Acknowledgements

This study was jointly funded by the State 973 Program of China (Grant No. 2012CB214704), the National S&T Major Project of

China (Grant No. 2011ZX05008-002-50) and National Natural Science Foundation of China (Grant No. 41172114). We thank Dr. An Xu of the Guangzhou Institute of Geochemistry and Dr. Guangyou Zhu of the Research Institute of Petroleum Exploration and Development, PetroChina for their kind help and support for this study. We thank Drs. Frank Mango and Ken Peters, and three anonymous reviewers for their critical comments, which substantially improved our manuscript. We are very grateful to Dr. Ken Peters for his language improvements and editorial work. This is contribution No. IS-1746 from GIGCAS.

Appendix A. Supplementary data

Supplementary data associated with this article can be found, in the online version, at http://dx.doi.org/10.1016/j.orggeochem.2013.09.004.

Associate Editor – **Ken Peters**

References

Alexander, R., Berwick, L.J., Pierce, K., 2011. Single carbon surface reactions of 1-octadecene and 2,3,6-trimethylphenol on activated carbon: implications for methane formation in sediments. Organic Geochemistry 42, 540–547.

Behar, F., Kressman, S., Rudkiewicz, J.L., Vandenbrouke, M., 1992. Experimental simulation in a confined system and kinetic modeling of kerogen and oil cracking. Organic Geochemistry 19, 173–189.

Behar, F., Vandenbroucke, M., Tang, Y., Marquis, F., Espitalié, J., 1997. Thermal cracking of kerogen in open and closed systems: determination of kinetic parameters and stoichiometric coefficients for oil and gas generation. Organic Geochemistry 26, 321–339.

Boreham, C.J., Horsfield, B., Schenk, H.J., 1999. Predicting the quantities of oil and gas generated from Australian Permian coals, Bowen Basin using pyrolytic methods. Marine and Petroleum Geology 16, 165–188.

Braun, R.L., Burnham, A.K., 1998. Kinetics GUI.exe, Version 1.11.

Cramer, B., 2004. Methane generation from coal during open system pyrolysis investigated by isotope specific, Gaussian distributed reaction kinetics. Organic Geochemistry 35, 379–392.

Dai, J., Wang, T., Song, Y., 1997. The Formation Conditions and Distribution Rules of Giant Gas Fields in China. Geology Press, Beijing (in Chinese).

Dai, J., Chen, J., Zhong, N., Pang, X., Qing, S., 2003. Giant Gas fields in China and their Genesis. Science Press, Beijing (in Chinese).

Dai, J., Li, J., Luo, X., Zhang, W., Hu, G., Ma, C., Guo, J., Ge, S., 2005. Stable carbon isotope compositions and source rock geochemistry of the giant gas accumulations in the Ordos Basin, China. Organic Geochemistry 36, 1617–1635.

Dai, J., Zou, C., Qin, S., Tao, S., Ding, W., Liu, Q., Hu, A., 2008. Geology of giant gas fields in China. Marine and Petroleum Geology 25, 320–334.

Dieckmann, V., 2005. Modelling petroleum formation from heterogeneous source rocks: the influence of frequency factors on activation energy distribution and geological prediction. Marine and Petroleum Geology 22, 375–390.

Dieckmann, V., Schenk, H.J., Horsfield, B., Welte, D.H., 1998. Kinetics of petroleum generation and cracking by programmed-temperature closed-system pyrolysis of Toarcian Shales. Fuel 77, 23–31.

Dieckmann, V., Schenk, H.J., Horsfield, B., 2000. Assessing the overlap of primary and secondary reactions by closed- versus open-system pyrolysis of marine kerogens. Journal of Analytical and Applied Pyrolysis 56, 33–46.

Dieckmann, V., Fowler, M., Horsfield, B., 2004. Predicting the composition of natural gas generated by the Duvernay Formation (Western Canada Sedimentary Basin) using a compositional kinetic approach. Organic Geochemistry 35, 845–862.

Dieckmann, V., Ondrak, R., Cramer, B., Horsfield, B., 2006. Deep basin gas: new insights from kinetic modeling and isotopic fractionation in deep-formed gas precursors. Marine and Petroleum Geology 23, 183–199.

Erdmann, M., Horsfield, B., 2006. Enhanced late gas generation potential of petroleum source rocks via recombination reactions: evidence from the Norwegian North Sea. Geochimica et Cosmochimica Acta 70, 3943–3956.

Greensfelder, B.S., Voge, H.H., Good, G.M., 1949. Catalytic and thermal cracking of pure hydrocarbons. Industrial and Engineering Chemistry 41, 2573–2584.

Hao, F., Guo, T., Zhu, Y., Cai, X., Zou, H., Li, P., 2008. Evidence for multiple stages of oil cracking and thermochemical sulfate reduction in the Puguang gas field, Sichuan Basin, China. American Association of Petroleum Geologists Bulletin 92, 611–637.

Hill, R.J., Tang, Y., Kaplan, I.R., 2003. Insight into oil cracking based on laboratory experiments. Organic Geochemistry 34, 1651–1672.

Hill, R.J., Zhang, E., Katz, B.J., Tang, Y., 2007. Modeling of gas generation from the Barnett Shale, Fort Worth Basin, Texas. American Association of Petroleum Geologists Bulletin 91, 501–521.

Horsfield, B., Schenk, H.J., Mills, N., Welte, D.H., 1992. Closed-system programmed-temperature pyrolysis for simulating the conversion of oil to gas in a deep petroleum reservoir. Organic Geochemistry 19, 191–204.

Lewan, M.D., Kotarba, M.J., Wiecław, D., Piestrzynski, A., 2008. Evaluating transition-metal catalysis in gas generation from the Permian Kupferschiefer by hydrous pyrolysis. Geochimica et Cosmochimica Acta 72, 4069–4093.

Liang, D., Zhang, S., Chen, J., Wang, F., Wang, P., 2003. Organic geochemistry of oil and gas in the Kuqa depression, Tarim Basin, NW China. Organic geochemistry 34, 873–888.

Liu, D., Liu, J., Peng, P., Shuai, Y., 2004. Carbon isotope kinetics of gaseous hydrocarbons generated from different kinds of vitrinites. Chinese Science Bulletin 49 (Supp. I), 72–78.

Liu, Q.Y., Worden, R.H., Jin, Z.J., Liu, W.H., Li, J., Gao, B., Zhang, D.W., Hu, A.P., Yang, C., 2013. TSR versus non-TSR processes and their impact on gas geochemistry and carbon stable isotopes in Carboniferous, Permian and Lower Triassic marine carbonate gas reservoirs in the Eastern Sichuan Basin, China. Geochimica et Cosmochimica Acta 100, 96–115.

Lorant, F., Prinzhofer, A., Behar, F., Huc, A.-Y., 1998. Carbon isotopic and molecular constraints on the formation and expulsion of thermogenic hydrocarbon gases. Chemical Geology 147, 249–264.

Mango, F.D., 1992. Transition metal catalysis in the generation of petroleum and natural gas. Geochimica et Cosmochimica Acta 56, 553–555.

Mango, F.D., 1997. The light hydrocarbons in petroleum: a critical review. Organic Geochemistry 26, 417–440.

Mango, F.D., 2001. Methane concentrations in natural gas: the genetic implications. Organic Geochemistry 32, 1283–1287.

Mango, F.D., Hightower, J.W., James, A.T., 1994. Role of transition-metal catalysis in the formation of natural gas. Nature 368, 536–538.

Mansuy, L., Landais, P., Ruau, O., 1995. Importance of the reacting medium in artificl maturation of a coal by confied pyrolysis. 1. Hydrocarbons and polar compounds. Energy & Fuels 9, 691–703.

McNeil, R.I., BeMent, W.O., 1996. Thermal stability of hydrocarbons: Laboratory criteria. Energy & Fuels 10, 60–67.

Monthioux, M., Landais, P., Monin, J.C., 1985. Comparison between natural and artificial maturation series of humic coals from the Mahakam Delta, Indonesia. Organic Geochemistry 8, 275–292.

Monthioux, M., Landais, P., Durand, B., 1986. Comparison between extracts from natural and artificial maturation series of Mahakam Delta coals. Organic Geochemistry 10, 299–311.

Pan, C., Yu, L., Liu, J., Fu, J., 2006. Chemical and carbon isotopic fractionations of gaseous hydrocarbons during abiogenic oxidation. Earth and Planetary Science Letters 246, 70–89.

Pan, C., Geng, A., Zhong, N., Liu, J., Yu, L., 2008. Kerogen pyrolysis in the presence and absence of water and minerals. Part 1. Gas components. Energy & Fuels 22, 416–427.

Pan, C., Jiang, L., Liu, J., Zhang, S., Zhu, G., 2010. The effects of calcite and montmorillonite on oil cracking in confined pyrolysis experiments. Organic Geochemistry 41, 611–626.

Pan, C., Jiang, L., Liu, J., Zhang, S., Zhu, G., 2012. The effects of pyrobitumen on oil cracking in confined pyrolysis experiments. Organic Geochemistry 45, 29–47.

Pelet, R., 1994. Comments on the paper "The effects of the mineral matrix on the determination of kinetic parameters using modified Rock-Eval pyrolysis" by H. Dembicki Jr., Organic Geochemistry, 18, 531–539 (1992). Organic Geochemistry 21, 979–981.

Pepper, A.S., 1992. Estimating of petroleum expulsion behavior of source rocks: a novel quantitative approach. In: England, A.J., Fleet, A.J. (Eds.), Petroleum Migration, vol. 59. Geological Society Special Publication, pp. 9–31.

Pepper, A.S., Dodd, T.A., 1995. Simple kinetic models of petroleum formation. Part II: oil-gas cracking. Marine and Petroleum Geology 12, 321–340.

Pepper, A.S., Corvi, P.J., 1995. Simple kinetic models of petroleum formation. Part III: modelling an open system. Marine and Petroleum Geology 12, 417–452.

Prinzhofer, A.A., Huc, A.Y., 1995. Genetic and post-genetic molecular and isotopic fractionations in natural gases. Chemical Geology 126, 281–290.

Sandvik, E.I., Young, W.A., Curry, D.J., 1992. Expulsion from hydrocarbon sources: the role of organic absorption. Organic Geochemistry 19, 77–87.

Schenk, H.J., Horsfield, B., 1993. Kinetics of petroleum generation by programmed-temperature closed- versus open-system pyrolysis. Geochimica et Cosmochimica Acta 57 (3), 623–630.

Schenk, H.J., di Primo, R., Horsfield, B., 1997. The conversion of oil into gas in petroleum reservoirs. Part 1: Comparative kinetic investigation of gas generation from crude oils of lacustrine, marine and fluviodeltaic origin by programmed temperature closed-system pyrolysis. Organic Geochemistry 26, 467–481.

Shuai, Y., Peng, P., Zou, Y., Zhang, S., 2006. Kinetic modeling of individual gaseous component formed from coal in a confined system. Organic Geochemistry 37, 932–943.

Smith, J.W., Batts, B.D., Gilbert, T.D., 1989. Hydrous pyrolysis of model compounds. Organic Geochemistry 14, 365–373.

Snowdon, L.R., 2001. Natural gas composition in a geological environment and the implications for the processes of generation and preservation. Organic Geochemistry 32, 913–931.

Sweeney, J.J., Burnham, A.K., 1990. Evaluation of a simple model of vitrinite reflectance based on chemical kinetics. American Association of Petroleum Geologists Bulletin 74, 1559–1570.

Tang, Y., Jenden, P.D., Nigrini, A., Teerman, S.C., 1996. Modeling early methane generation in coal. Energy & Fuels 10, 659–671.

Tang, Y., Perry, J.K., Jenden, P.D., Schoell, M., 2000. Mathematical modeling of stable carbon isotope ratios in natural gases. Geochimica et Cosmochimica Acta 64, 2673–2687.

Tian, H., Xiao, X., Wilkins, R.W.T., Tang, Y., 2012. An experimental comparison of gas generation from three oil fractions: implications for the chemical and stable carbon isotopic signatures of oil cracking gas. Organic Geochemistry 46, 96–112.

Tissot, B.P., Welte, D.H., 1984. Petroleum Formation and Occurrence. Springer Verlag, Berlin.

Tsang, W., 1989. Rate constants for the decomposition and formation of simple alkanes over extended temperature and pressure ranges. Combustion and Flame 78, 71–86.

Ungerer, P., Pelet, R., 1987. Extrapolation of the kinetics of oil and gas formation from laboratory experiments to sedimentary basins. Nature 327, 52–54.

Vu, T.A.T., Horsfield, B., Sykes, R., 2008. Influence of in-situ bitumen on the generation of gas and oil in New Zealand coal. Organic Geochemistry 39, 1606–1619.

Waples, D.W., 2000. The kinetics of in-reservoir oil destruction and gas formation: constraints from experimental and empirical data, and from thermodynamics. Organic Geochemistry 31, 553–575.

Xiao, X.M., Zeng, Q.H., Tian, H., Wilkins, R.W.T., Tang, Y.C., 2005. Origin and accumulation model of the AK-1 natural gas pool from the Tarim Basin, China. Organic Geochemistry 36, 1285–1298.

Xiao, X.M., Xiong, M., Tian, H., Wilkins, R.W.T., Huang, B.J., Tang, Y.C., 2006. Determination of the source area of the Ya13-1 gas pool in the Qiongdongnan Basin, South China Sea. Organic Geochemistry 37, 990–1002.

Xiao, X.M., Li, N.X., Gan, H.J., Jin, Y.B., Tian, H., Huang, B.J., Tang, Y.C., 2009. Tracing of deeply-buried source rock: a case study of the WC9-2 petroleum pool in the Pearl River Mouth Basin, South China Sea. Marine and Petroleum Geology 26, 1365–1378.

Xiong, Y., Geng, A., Liu, J., 2004. Kinetic-simulating experiment combined with GCIRMS analysis: application to identification and assessment of coal-derived methane from Zhongba Gas Field (Sichuan Basin, China). Chemical Geology 213, 325–338.

Zhao, M., Lu, S., Wang, T., Li, J., 2002. Geochemical characteristics and formation process of natural gas in the Kela 2 gas field. Chinese Science Bulletin 47, 113–119.

Zhao, W., Zhang, S., Wang, F., Cramer, B., Chen, J., Sun, Y., Zhang, B., Zhao, M., 2005. Gas systems in the Kuche Depression of the Tarim Basin: source rock distributions, generation kinetics and gas accumulation history. Organic Geochemistry 36, 1583–1601.